Chapter 4

Non-viral vectors based on arginino-calix[4]arenes

4.1 Introduction

It is well known that arginine (**Fig. 4.1**) is the most basic of all natural amino acids, followed by lysine and histidine.

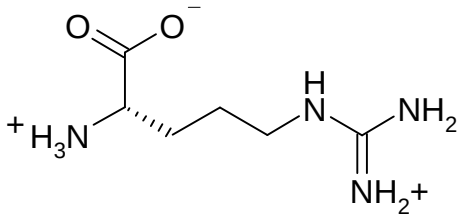

Fig. 4.1. Structural formula of the amino acid arginine in solution at neutral pH.

Arginine owes the basicity to its guanidine moiety in the side chain, which is protonated at neutral pH. In its free form or built into peptides, proteins, or receptor systems, it is capable of forming both electrostatic and directed hydrogen bond interactions with polar and anionic molecules, mainly through its planar, fork-like guanidinium functionality. Resonance stabilization of the molecule spreads the positive charge evenly on the three nitrogen atoms and guanidine, which by itself has a p*K*a of 13.5 in water, is characterized in the arginine by a p*K*a value attenuated to 12.5.[1]

The arginine residue and its function as anion binding site are ubiquitous in nature. It is found in the binding region of a large number of enzymes and signalling proteins, which employ this amino acid, and more specifically its guanidinium group, to interact forming strong ion-pairs with negatively charged oxoanions[2] such as carboxylates (**Fig. 4.2**) or phosphates. It interacts also with π-electron-rich aromatic units[3] and contributes to the stabilisation of protein tertiary structures via internal salt bridges.[4]

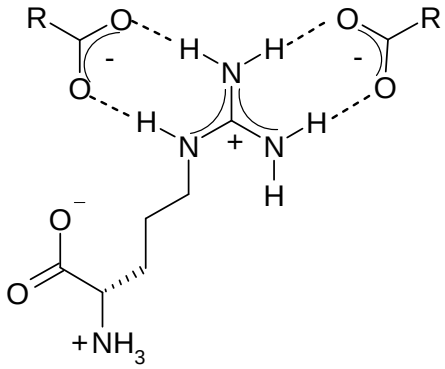

Fig. 4.2. The guanidinium group of arginine and its two possible binding patterns with carboxylate anions.

In particular, the interaction at the interface between two proteins has been found to include a disproportionately large number of arginine units, located in sites called “hot spots” in recent

literature discussions.[5] Moreover, protein-protein hetero-dimerization processes are often mediated by salt bridges involving arginine on one of the macromolecules and phosphorylated amino acids on the other. For example, phosphorylation of the OH group of a serine residue in a receptor enables the simultaneous interaction with two adjacent arginine residues of another receptor. On the other hand, phosphorylation of serines (or threonines) adjacent to the arginines of the same molecule slows down the attraction between the receptors.[6] Arginine is also involved in cell-cell and cell-matrix adhesion motifs such as RGD (arginine-glycine-aspartate). Adhesive proteins like fibronectin, osteopontin, vitronectin and collagens display the RGD sequence at their cell recognition site in extracellular matrices,[7] which is recognized by at least one member of the structural related integrins, a family of α,β hetero-dimeric transmembrane cellular receptors.[8]

Arginine peptides are also able to inhibit the NO synthase (NOS), which is the enzyme in charge of the nitrogen oxide (NO) synthesis. NO is enzimatically synthesized in many tissues and cell types starting from arginine.[9] Generally, molecules able to bind the enzyme in the active site deputy to the arginine binding are used as NOS inhibitors, blocking in this way the enzymatic activity.

Arginine is again essential in some proteins that interact with nucleic acids. These proteins are necessary for the control of the genetic information, replication, packaging and protection. In the nucleosome, in which the DNA winds around the arginine-rich histone, the positively charged amino acid side chains clearly show a direct interaction with the DNA phosphodiester skeleton.[10] Methylation of arginine residues in the histone core leads to a conformational change allowing DNA transcription,[11] that, in this way, can be regulated.

For the purpose of this thesis, arginine results of interest in particular for its involvement in cell penetration processes, a function which was discovered during studies on protein encoder by the human immunodeficiency virus type 1 (HIV-1) genome. A protein named Tat (transactivator of HIV transcription) was found to have the ability to internalize into cells,[12] binding the transactivation response element (TAR) of viral RNA and transactivating the viral promoter.[13] In 1994, it was reported that chemical conjugates of peptide segments derived from the Tat protein with other exogenous proteins allowed their internalization into cells.[14] It was later discovered that the arginine-rich segment GRKKRRQRRRPPQ in the Tat protein (positions 48-60) plays a fundamental role in the internalization of the exogenous proteins.[15]

Tat peptide indicated as TAT (48-60) is highly hydrophilic and basic, containing six arginines and two lysines. Delivery to and cell uptake of recombinant proteins having the shorter arginine-rich peptide TAT (47-57) fused with cargo were observed and, once inside the cell,

these chimaeras influenced its physiology.[16] The effect of the arginines number on the internalization efficiency was studied using the peptide composed only of arginine residues (Rn; n= 4, 8, 16).[17] Although no significant internalization was observed for the R4 peptide, both the R8 and R16 peptides showed efficient internalization. These results not only demonstrated the importance of arginine residues in the internalization of the Tat segment, but strongly suggest that novel simple intracellular delivery vectors composed only of arginines could be created. The importance of arginine residues for these purposes was also highlighted by Rothbard, Wender and coworkers.[18]

After these first results many other structural changes on this sequence were performed. Replacing all non-arginine residues in the Tat nonamer with arginines provides transporters that exhibit superior rates of uptake; charge itself is necessary but not sufficient because lysine nonamers show poor uptake[19] whereas the number of arginines is important, with optimal uptake being observed for oligomers of 7-15 residues.[19a,20] Backbone chirality is not critical for uptake and even the position of attachment and length of the side chains can be altered, as shown with guanidinium-rich peptoids that exhibit highly efficient uptake.

Changes in the backbone composition and side-chains spacing can also increase internalization.[18d,19b,21] The proximity of cations in these oligo-polymers results in charge repulsion and in order to minimize it in neutral water, anion scavenging is needed which eventually forms complexes with new physical properties. Full loading with monoanions or partial complexation with dianions will cause charge neutralization, extensive complexation with dianions charge inversion. Charge neutralization will increase the lipophilicity of guanidinium oligo-polymers so they can become soluble in hydrophobic solvents as long as a synergistic mixture of hydrophilic and amphiphilic anions is present. It is also possible to use the same, deceivingly hydrophilic polycation to mediate the translocation of anions across bulk and lipid bilayer membranes under the same conditions. Guanidinium-rich oligo/polymers, therefore, are both hydrophilic and lipophilic, depending on their counteranions environment.[22] Upon encountering a cell surface, the highly polar and water soluble oligoguanidinium transporters associate with cell surface bidentate hydrogen-bond acceptors that bear a complementary charge, such as carboxylates, phosphates and sulfates. This association converts the once polar oligoguanidinium transporter into a less polar ion-pair complex that is non covalently associated with the cell surface. Arginine rich transporters have also been used to translocate metals and imaging agents such as 40 nm iron beads[23] and ^{99m}Tc,[24] contrast agents (Gd chelates)[25] and to breach tissue barriers,[26] and may contribute to the modes of action of pore-forming R-rich natural antibiotics.[27]

These considerations brought to the use of the arginine unit also in the preparation of non viral vectors for gene delivery such as polyarginine,[28] dendrimers,[29] cell penetrating peptides (CPP),[30] PNA[31] and Gemini surfactants.[32]

Besides the guanidinium group, C-conjugated arginine is obviously characterized by the presence of the α-amino group which, if not involved in a bond lowering its basicity, could carry a further positive charge at proper pH conditions. In the possible use of this amino acid to bind DNA, this additional positive charge could result in a stronger interaction with the negative charges of the phosphate residues of the double helix, a better capacity to condense the DNA, a more efficient penetration of the cell membrane and in the "proton sponge" effect.[33] This latter effect consists in the vector ability of buffering the pH, due to the presence of amines with different basicity, which contrasts the acidity increase in the endosome, otherwise used by the cell to start the lisosomal degradation of the lipoplex, considered extraneous. The DNA-vector complex wholly covered by positive charges, interacting with the cell membrane, will determine a high local concentration of vector in the endosome. During the intracellular trafficking, the buffering capacity of the amines will not only tend to inhibit the action of the lysosomal nucleases that have an acid optimal pH, but will also alter the osmolarity of the vesicle. The accumulation of protons brought in by the endosomal ATPase is coupled to an influx of chloride anions. In the presence of these amines there will be a large increase in the ionic concentration within the endosome resulting in its osmotic swelling and rupture. For gene therapy the interesting aspect of this mechanism, somewhat primitive compared to the mechanisms developed by viruses, is that it will lead to enhanced gene transfer, as the DNA introduced with the vector will be rapidly liberated from the damaging endosomal environment creating an escape mechanism for the polycation/DNA particles.[34]

On these bases we considered the possibility of replacing the simple guanidinium groups on the calixarene scaffold with arginine units suitably linked to the macrocycle structure.

Ungaro's research group started to investigate the functionalisation of the upper rim[35] of calix[4]arenes with amino acids obtaining first the *N-linked*-peptidocalix[4]arenes.[36] Subsequently the conjugation occurred through the amino acid carboxy groups and the first *C-linked*-peptidocalixarenes[37] were synthesized. These hybrid receptors are characterised by the presence of polar, hydrogen bonding moieties in close proximity to the calixarene apolar cavity, which, in principle, should shift the molecular recognition properties of native calixarenes toward more polar neutral guests and ions.[38] Moreover, they could also interact, in a multivalent fashion,[39] with biological targets or self-assemble through hydrogen bonding,

giving novel supramolecular architectures and enlarging the scope of calixarenes in Supramolecular Chemistry.

There are only few examples in which the arginine unit was introduced in a calixarene scaffold, and none of them is finalized to gene delivery or cell penetration. In the first example a calix[4]arene was derivatized with an RGD motif at the upper rim (**Fig. 4.3**) via solid phase synthesis, to obtain a potential integrin inhibitor.[40]

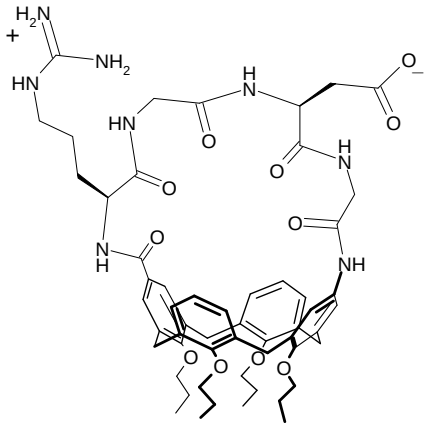

I

Fig. 4.3. Structural formula of RGD containing calix[4]arene **I** studied as a potential integrin inhibitor.

In the second example[41] (**Fig. 4.4**) the amino acid was not coupled directly to the calixarene backbone. Arginine was used to improve the performance of [2]rotaxanes as mimics of protein binding domains, in which one blocking group was replaced with a calix[4]arene.

The calix[4]arene provides the necessary hydrophobic pocket for strong association in aqueous solutions, and the rotaxane ring was envisioned as a crude mimic of an antibody hypervariable loop.

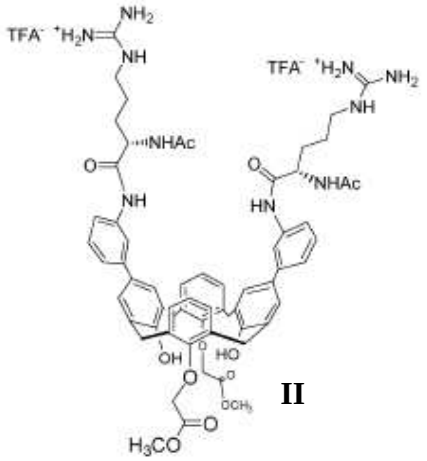

II

Fig. 4.4. Structural formula of an arginine containing calix[4]arene **II** studied as [2]rotaxane component.[41]

Acetyl-protected arginines were used as the recognition elements because they are a key residue in protein binding domains[5] and contain a chiral center that could potentially provide diastereomeric complexes with chiral guests.

In the third example[42] the arginine is directly bound to the upper rim of a calix[4]arene, *via* its amino group (**Fig. 4.5**) and the compounds used to block potassium channels.

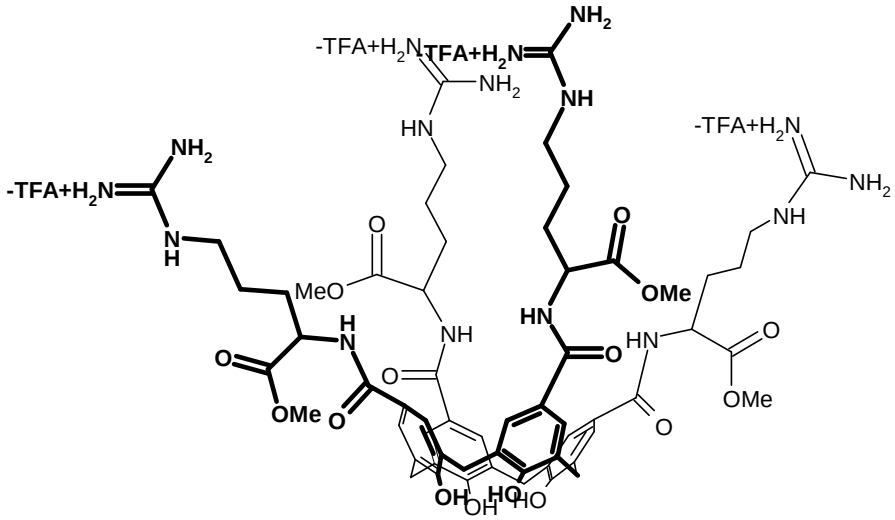

III

Fig. 4.5. Structural formula of calix[4]arene **III** studied as channel blockers. R^1= CO-Arg-OMe^+ TFA^-, R^2 = R^3 = H.

Potassium channels are major targets in biomedical and pharmacological research, because many diseases, mostly nervous disturbances, are linked to these membrane proteins.[43] The fact that >90 genes for different K^+ channel subunits have been so far identified in the human genome constitutes a major challenge in the development of ligands that specifically bind a certain channel subtype.[44] Calix[4]arenes displaying conical shapes that would likely complement the shape of the outer vestibule of a K_v channel were synthesised,[42] derivatized at the upper rim with cationic substituents, also guanidines and arginine units, to ideally complement the mainly negatively charged extracellular surface groups of the channel at the "turret loop".

With the aim of finding out potential vectors with better performances in terms of transfection efficiency and low toxicity, the work described in this chapter was devoted to the synthesis of calix[4]arenes derivatized with arginine units at the upper and lower rim, to study their biological properties and compare them with the corresponding analogues derivatized only with the guanidinium group. To reach this goal, previously reported reaction procedures to derivatize the calixarenes with amino acids and small peptides and routine peptide chemistry

have been used. The arginine residues were coupled by their carboxylic group, leaving free the amino group in order to exploit it for the useful effects mentioned before.

4.2 Results

4.2.1 Synthesis of upper rim arginine-calix[4]arene conjugates

Two upper rim arginine-calix[4]arene conjugates (arginino-calix[4]arenes) (**Fig. 4.6**) were synthesized, with different alkyl chains at the lower rim, hexyl for **59**, and ethoxyethyl for **63**, to evaluate also the effect of a subtle change in the polarity of the lower portion of the molecule on the vector properties.

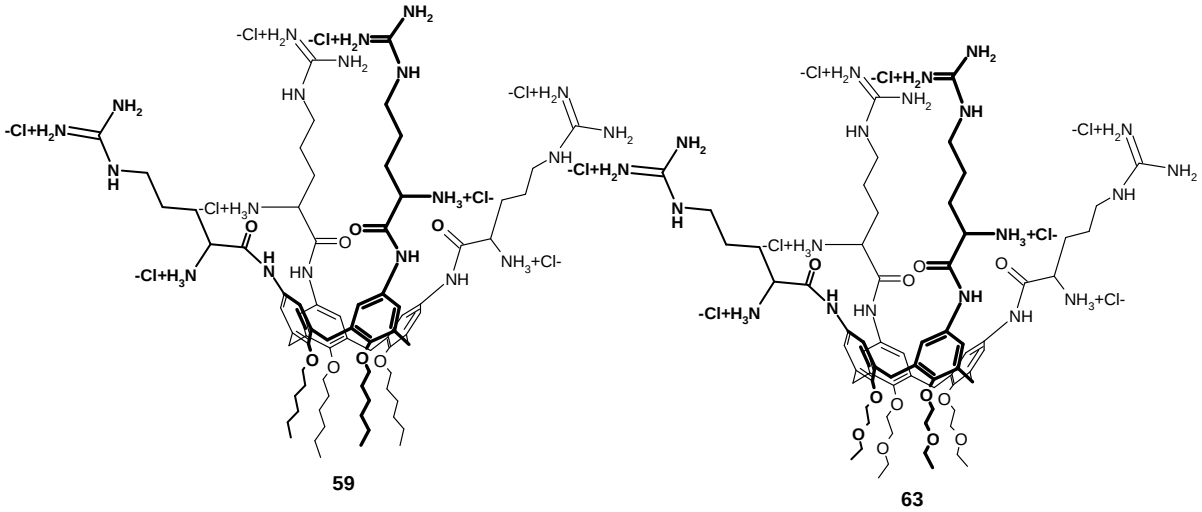

Fig. 4.6. Upper rim arginino-calix[4]arenes synthesized.

The general strategy adopted to synthesize compounds **59** and **63** substantially consisted in two steps (**Scheme 4.1**): the coupling of the arginine, conveniently protected on the amino and guanidino groups, with the amino-calix[4]arene derivative **56**, followed by deprotection. The success of this reaction scheme was tightly dependent on the nature of the protecting groups used for the amino acid N-atoms. In the coupling reaction HOBt and DCC were used as typical coupling reagents and in all cases a big problem encountered was the dicyclohexylurea (DCU) removal from the reaction medium. Since it is not completely insoluble in organic media, DCU could be only partially removed by filtration at the end of the reaction. Moreover, a N-acylurea by-product (**Fig. 4.7**), formed through an O-acylisourea rearrangement of the intermediate from the DCC and the amino acid,[45] was produced in substantial amount.

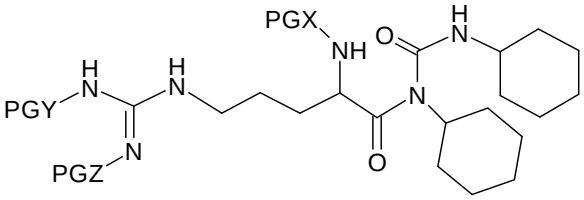

Fig. 4.7. N-acylurea by-product.

Another by-product formed, with a lower molecular weight with respect to the expected tetrafunctionalized derivative and detected in the ESI-MS spectrum, but it did not correspond to the trifunctionalized compound.

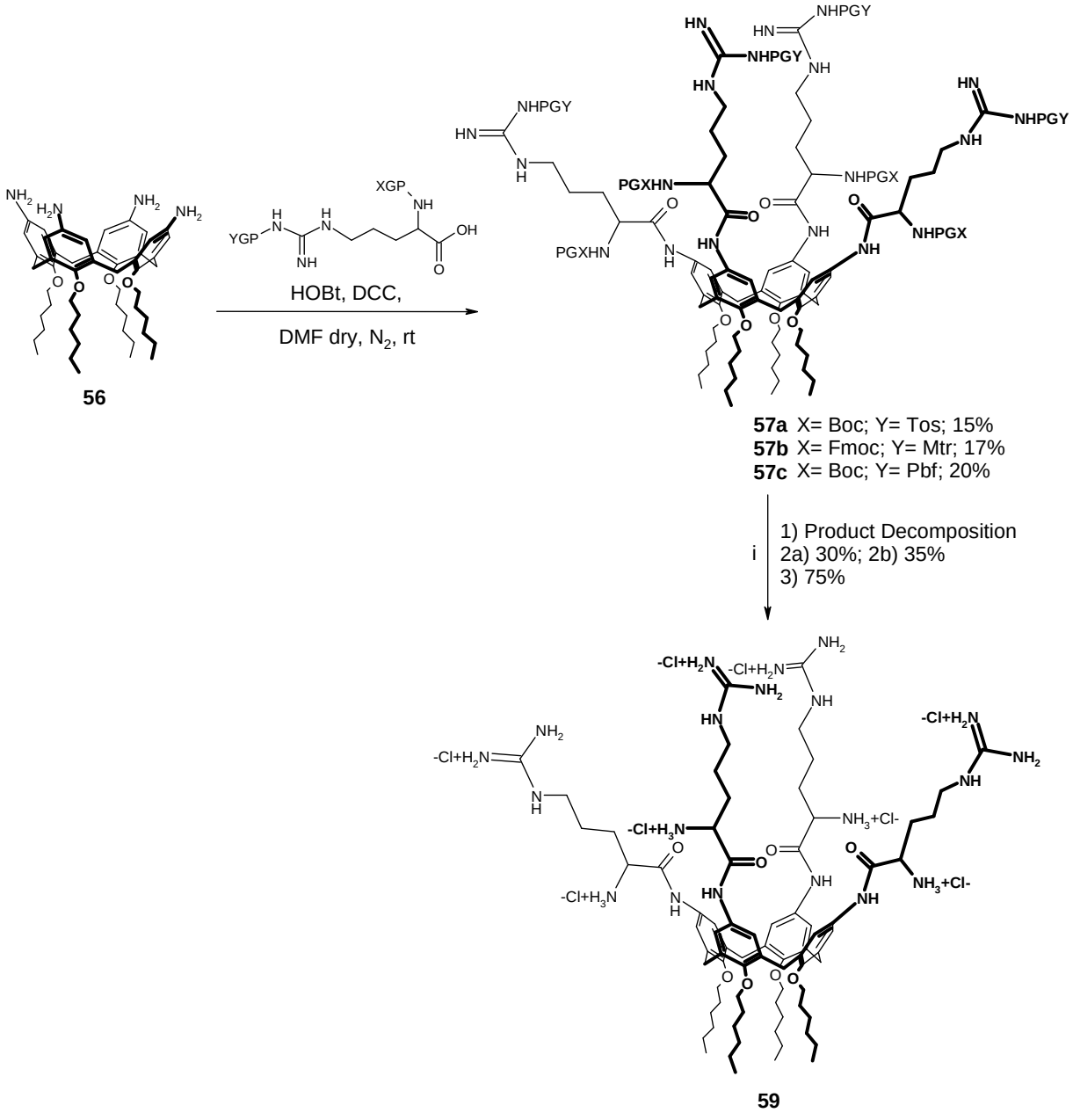

Scheme 4.1. Synthesis of **59**. i) 1) TFA, TFMSA, m-cresol, thioanisole, rt; 2a) piperidine, dry DCM, N_2, rt; 2b) TFA, TIS, H_2O, dil HCl, rt; 3) TFA, TIS, H_2O, dil HCl, rt.

Both these by-products and DCU must be removed from the crude product by column chromatography or preparative TLC plates. First the Boc-Arg(Tos)-OH was used and the conjugated product **57a** was obtained in moderate yields, because this compound is strongly absorbed on silica gel and could not be quantitatively recovered. Its ^{1}H NMR spectrum (**Fig. 4.8**) proved the success of the coupling reaction. Deprotection of **57a** was performed using a literature method[46] which employs the following reagents: TFA/TFMSA/m cresol/thioanisole (6:2:1:1). At the end of the reaction precipitation with diethyl ether and centrifugation to remove the scavengers were performed.

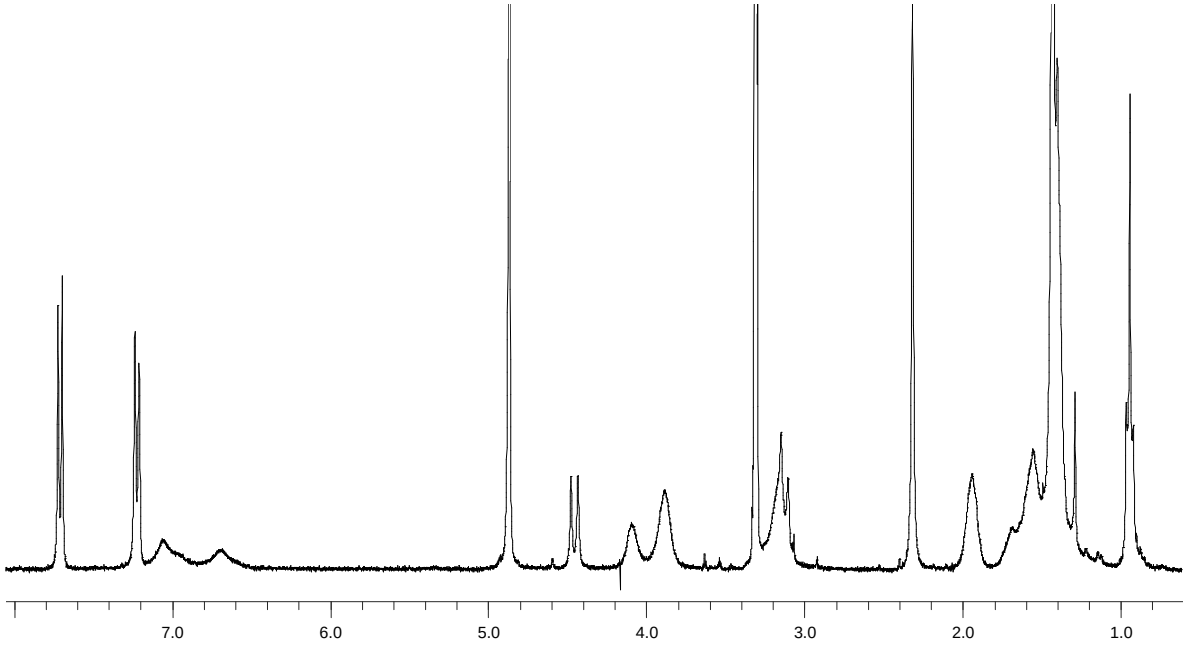

Fig. 4.8. ^{1}H NMR spectrum ($CDCl_3/CD_3OD$ = 19:1, 300 MHz, 298 K) of compound **57a**.

The precipitate was analyzed by ^{1}H NMR and it resulted to be arginine alone. Therefore, it was concluded that the strong acidic conditions break the amide bonds at the upper rim, and the amino-calixarene **56** goes into diethyl ether solution. This reaction could be due to an enhanced reactivity of the amide bond on the calix[4]arene, because it does not occur, for example, when the arginine is inserted in a PNA.[46] To skip these conditions, Fmoc-Arg(Mtr)-OH was used as an alternative, because the Mtr group is removed in a milder way than the Tosyl one.

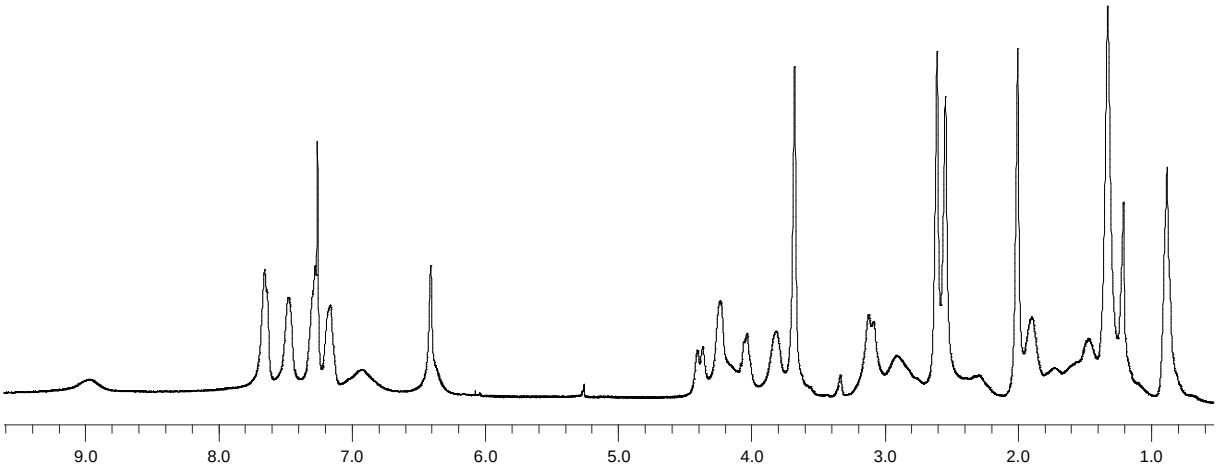

Fig. 4.9. ^{1}H NMR spectrum ($CDCl_3/CD_3OD$ = 19/1, 300 MHz, 298 K) of compound **57b**.

The coupling reaction was successful and the product **57b** was characterized by ^{1}H NMR (**Fig. 4.9**).

Concerning the deprotection of compound **57b**, the procedure consists first in the removal of the Fmoc groups, through reaction with piperidine, obtaining **58**. The deprotection was followed by ESI-MS (data not reported).

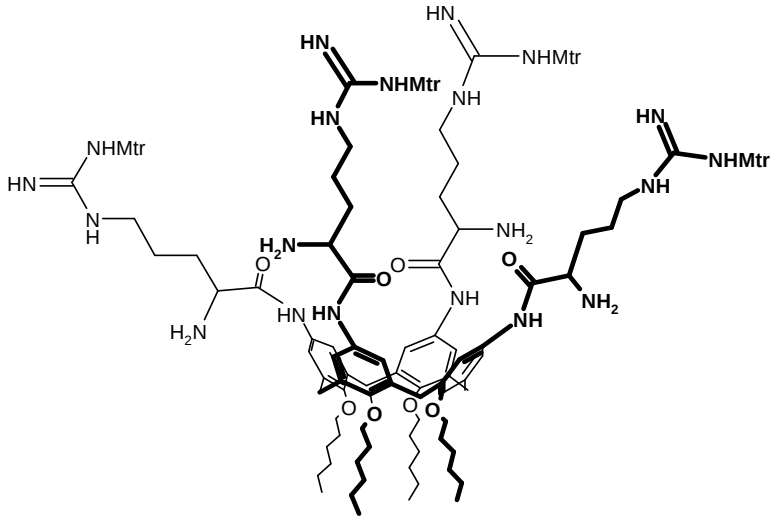

58

The compound **58** was further deprotected from Mtr with a solution of TFA (95%), TIS (2.5%) and H_2O (2.5%). After completion checked by ESI-MS, the crude product was dissolved in a solution of 1 M HCl and washed with dichloromethane to remove the scavengers and to convert the TFA-counterion into chloride, preferable for the biological tests and to increase the solubility in water of the molecule. The product coming from the ion exchange was analyzed by ^{1}H NMR (**Fig. 4.10**) and by ESI-MS (**Fig. 4.11**).

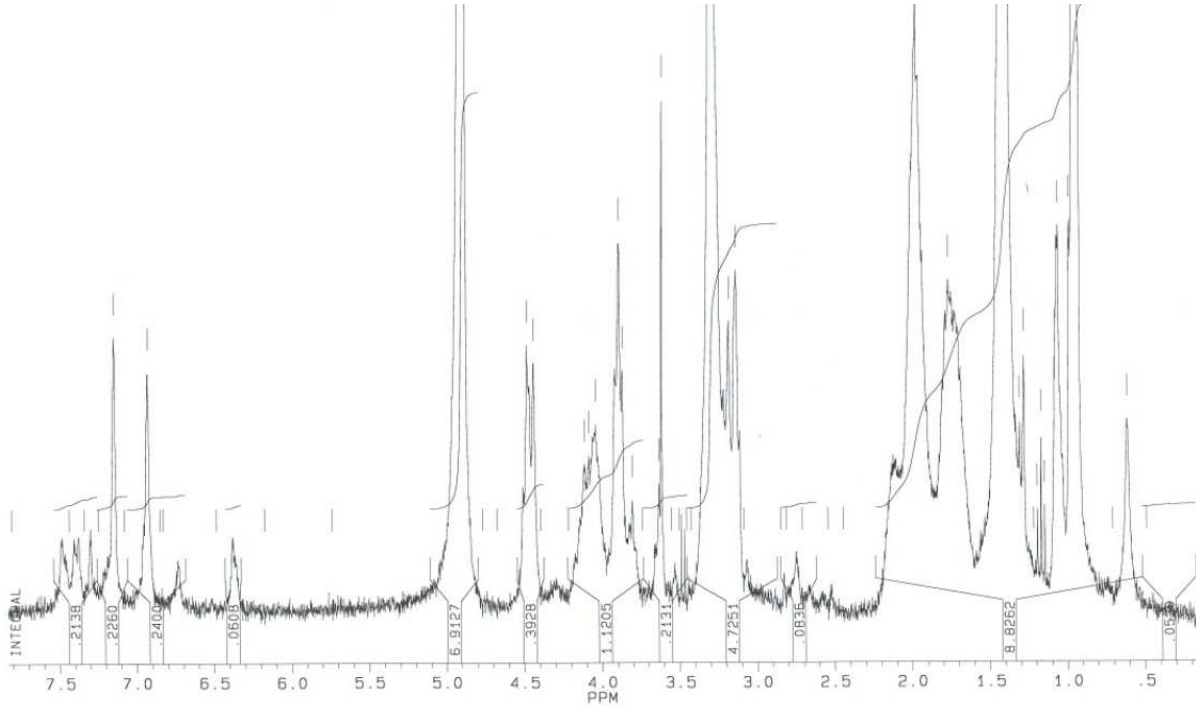

Fig. 4.10. ^{1}H NMR spectrum (CD_3OD, 300 MHz, 298 K) of the crude reaction product **59**, after deprotection of **58**.

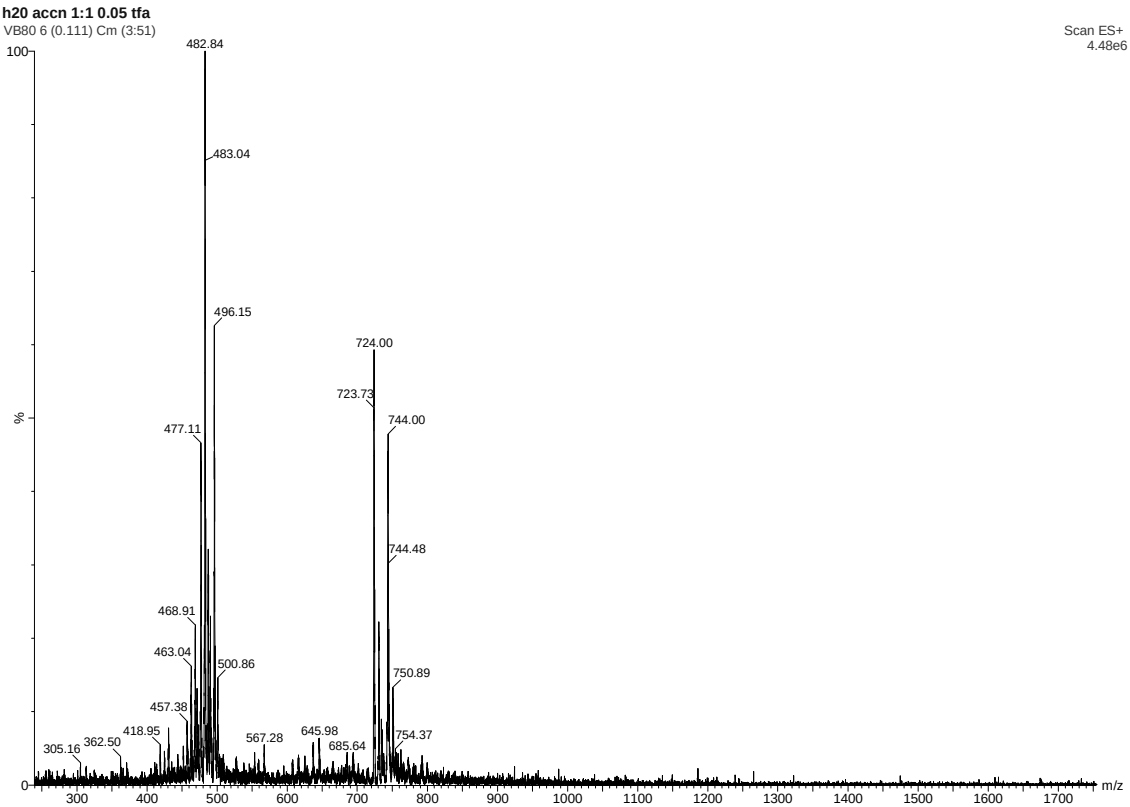

Fig. 4.11. ESI-MS spectrum of the crude reaction product **59**, after deprotection of **58**.

Unfortunately, in the aromatic area it was immediately noticeable that there were some signals related to a calixarene impurity, the presence of which was confirmed in the mass

spectrum (**Fig. 4.11**). In fact, besides the peaks at m/z 482.8 and 725.0, relative to the desired product **59** as $[M + 3H]^{3+}$ and $[M + 2H]^{2+}$ respectively, other ions at m/z 496.1 and 744.0 are present, corresponding to an impurity whose structure is at the moment still unknown.

Thanks to its solubility in water and acetonitrile the crude product could be analyzed by HPLC, a technique quite uncommon for molecules like calixarenes,[47] obtaining a trace with two peaks (**Fig. 4.12**).

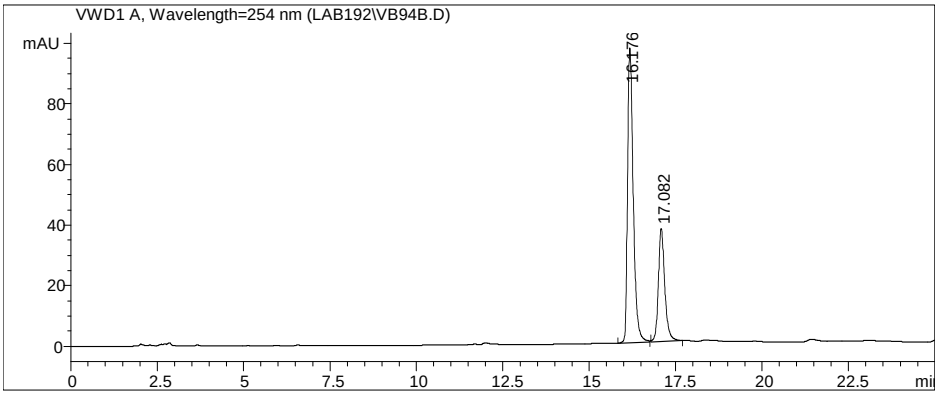

Fig. 4.12. HPLC trace of the crude reaction product **59**, after deprotection of **58**, analyzed on the C_{12} analytical column.

The mass analysis of the two separated fractions (**Fig. 4.13** and **4.14**), by direct injection of the collected fractions in the electrospray MS spectrometer and by HPLC-MS analysis, revealed that the correct product **59** is the one with the shorter retention time.

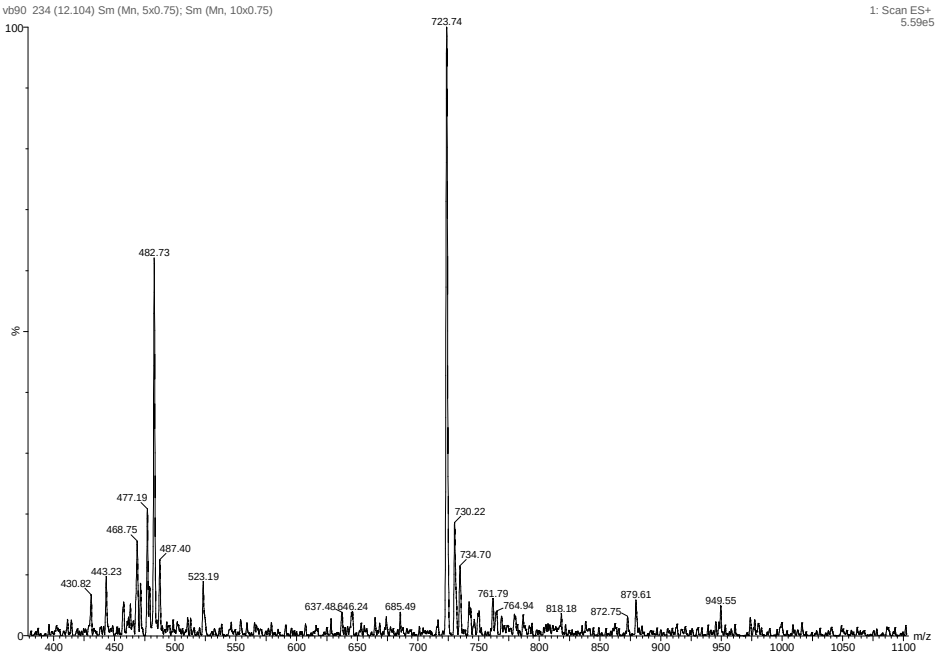

Fig. 4.13. ESI-MS spectrum of the first fraction collected, corresponding to the desired product **59**.

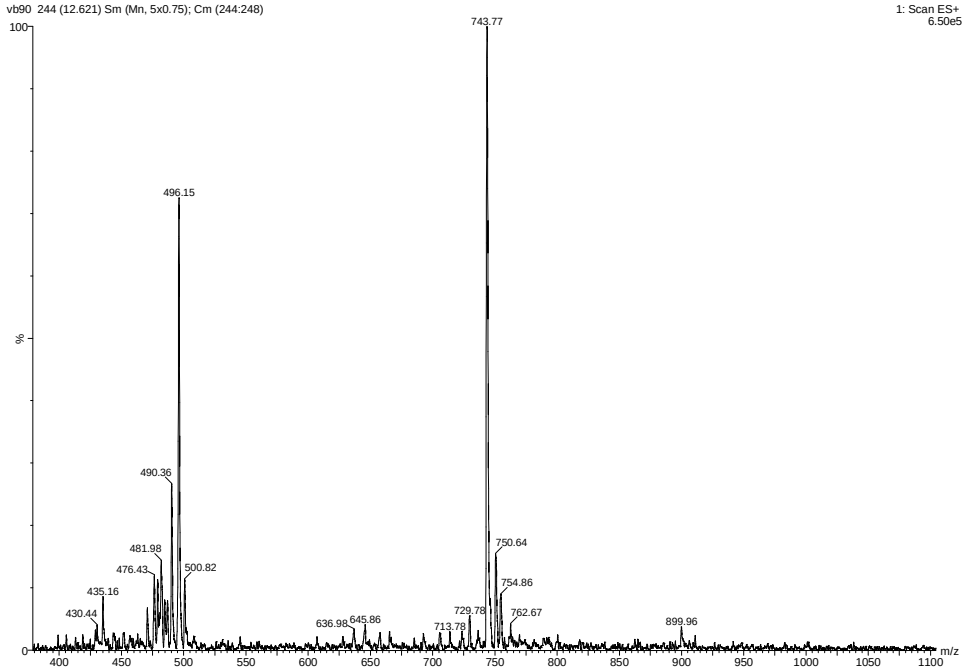

Fig. 4.14. ESI-MS spectrum of the second fraction collected, corresponding to the impurity.

The same profile was confirmed performing the purification by semipreparative HPLC (**Fig. 4.15**), in which the peptidocalixarene **59** was collected after 13.6 min.

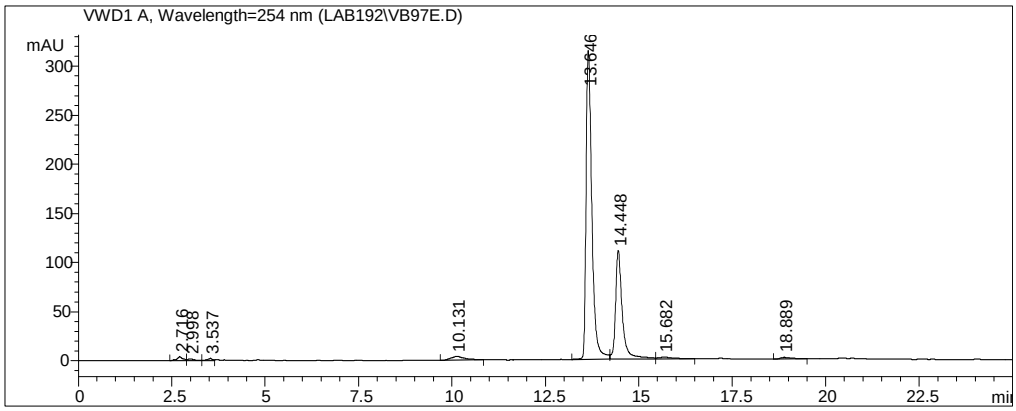

Fig. 4.15. HPLC trace of the crude reaction product **59**, after deprotection of **58**, analyzed on the C_{12} semipreparative column.

After the purification, the TFA-counterion was exchanged by adding 10 mM HCl to finally convert the compound into the chloride salt, which was analyzed by ^{1}H NMR in CD_3OD (**Fig. 4.16**).

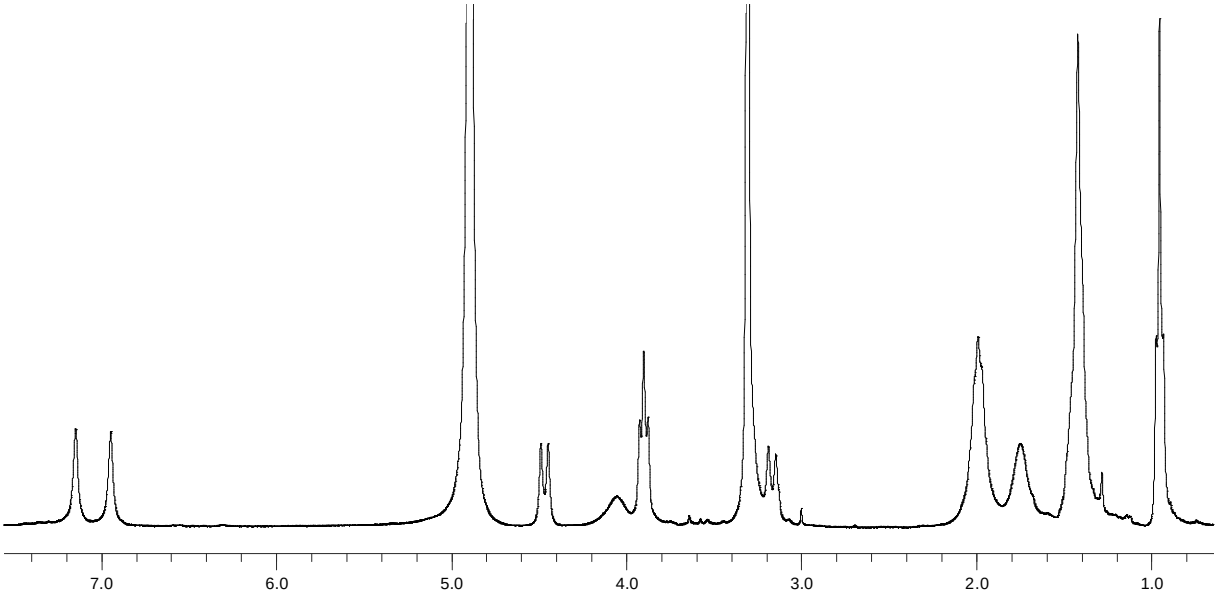

Fig. 4.16. ^{1}H NMR spectrum (CD_3OD, 300 MHz, 298 K) of compound **59**.

So this strategy brought to the desired product **59** but in low yield and after a long and difficult purification.

In order to improve the synthesis, Boc-Arg(Pbf)-OH was finally tested because it offers the possibility to remove both the Boc and Pbf protecting groups in one step, and in a mild way. The coupling reaction product **57c** was identified by ^{1}H NMR (**Fig. 4.17**) and subsequently deprotected in the same conditions used to remove the Mtr group. The work-up was done by precipitation in diethyl ether, centrifugation and washing with diethyl ether. The TFA-counterion was exchanged by adding 10 mM HCl in methanol to give successfully **59** in an easy way and in good yield.

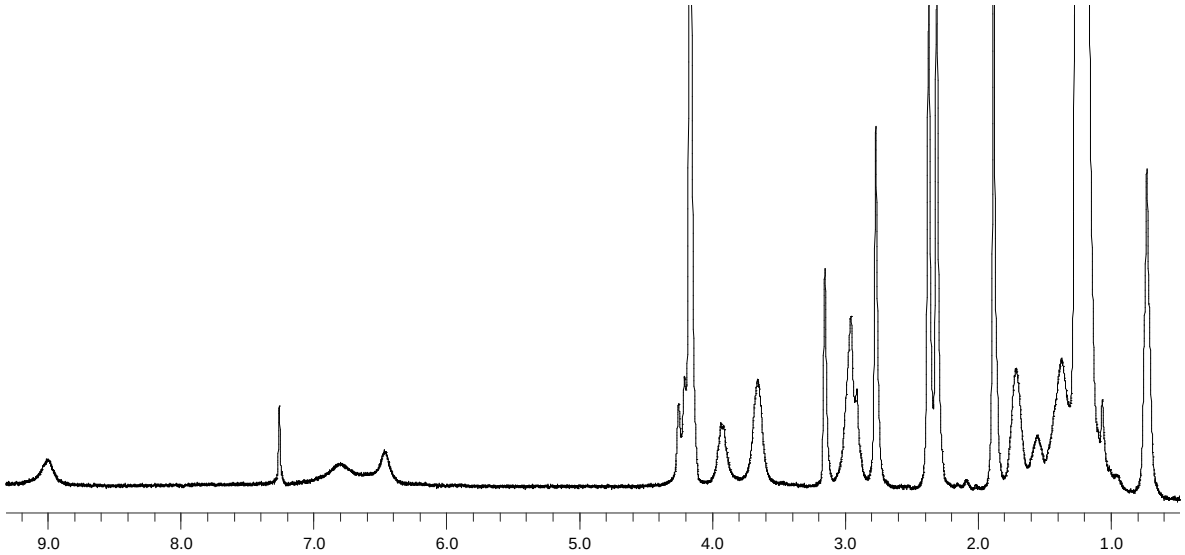

Fig. 4.17. ^{1}H NMR spectrum ($CDCl_3/CD_3OD$ = 19:1, 300 MHz, 298 K) of compound **57c**.

To evaluate the importance of the polarity of the alkyl chains, in the interaction with DNA and in the transfection efficiency, arginino-calixarene **63** having ethoxyethyl chains at the lower rim and arginine units at the upper rim was successfully synthesized. The strategy and the reaction conditions are the same used before for compound **59** and starting from the tetranitro derivative **60** (**Scheme 4.2**), obtained by ipso nitration of the known p-*t*-butyl precursor.[48]

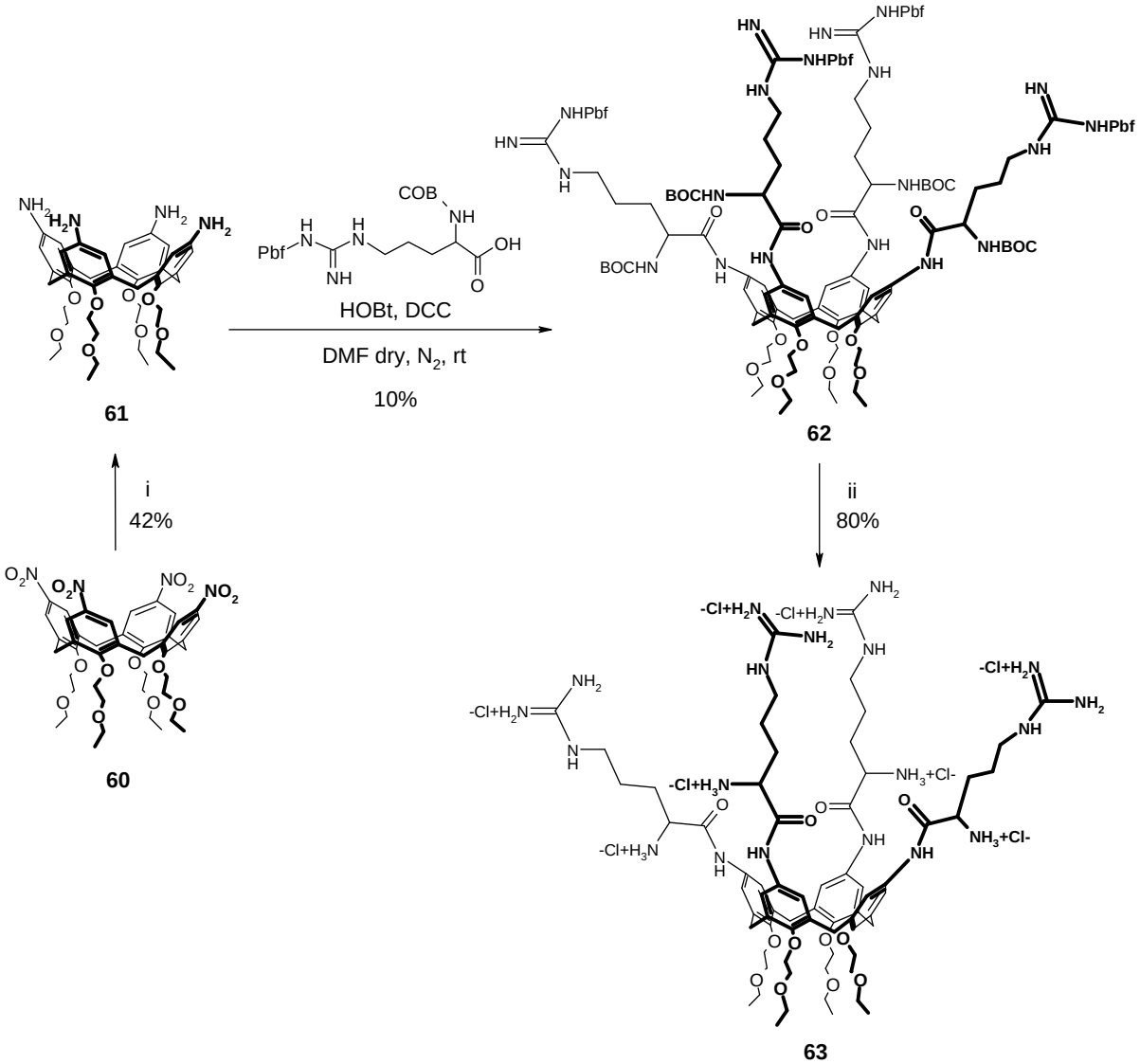

Scheme 4.2. Synthesis of **63**. i) $NH_2NH_2 \cdot H_2O$, Pd/C (10%), abs EtOH, N_2, reflux; ii) TFA, TIS, H_2O, dil HCl, rt.

4.2.2 Synthesis of a lower rim arginino-calix[4]arene

In view of the good results in terms of biological activity obtained with the guanidinium calix[4]arene **5b** (see **Paragraph 2.2.4**), it was also designed the synthesis of the correspondent lower rim arginino-calix[4]arene **66** (**Fig. 4.18**). The synthetic strategy started

from the amine **3b** which can be coupled with the carboxylic acid of the protected amino acid in presence of HOBT and DCC (**Scheme 4.3**).

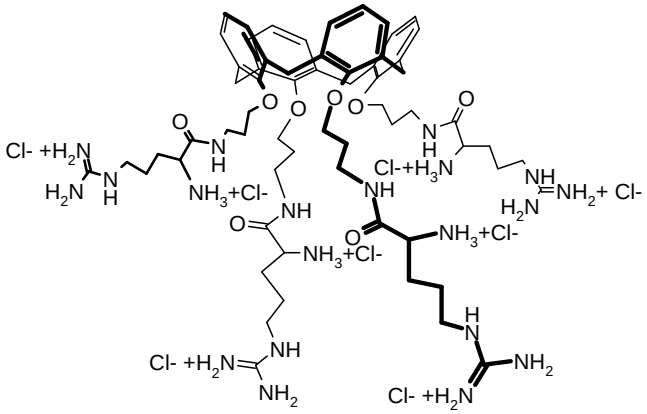

66

Fig. 4.18. Structural formula of lower rim arginine-calix[4]arene **66**.

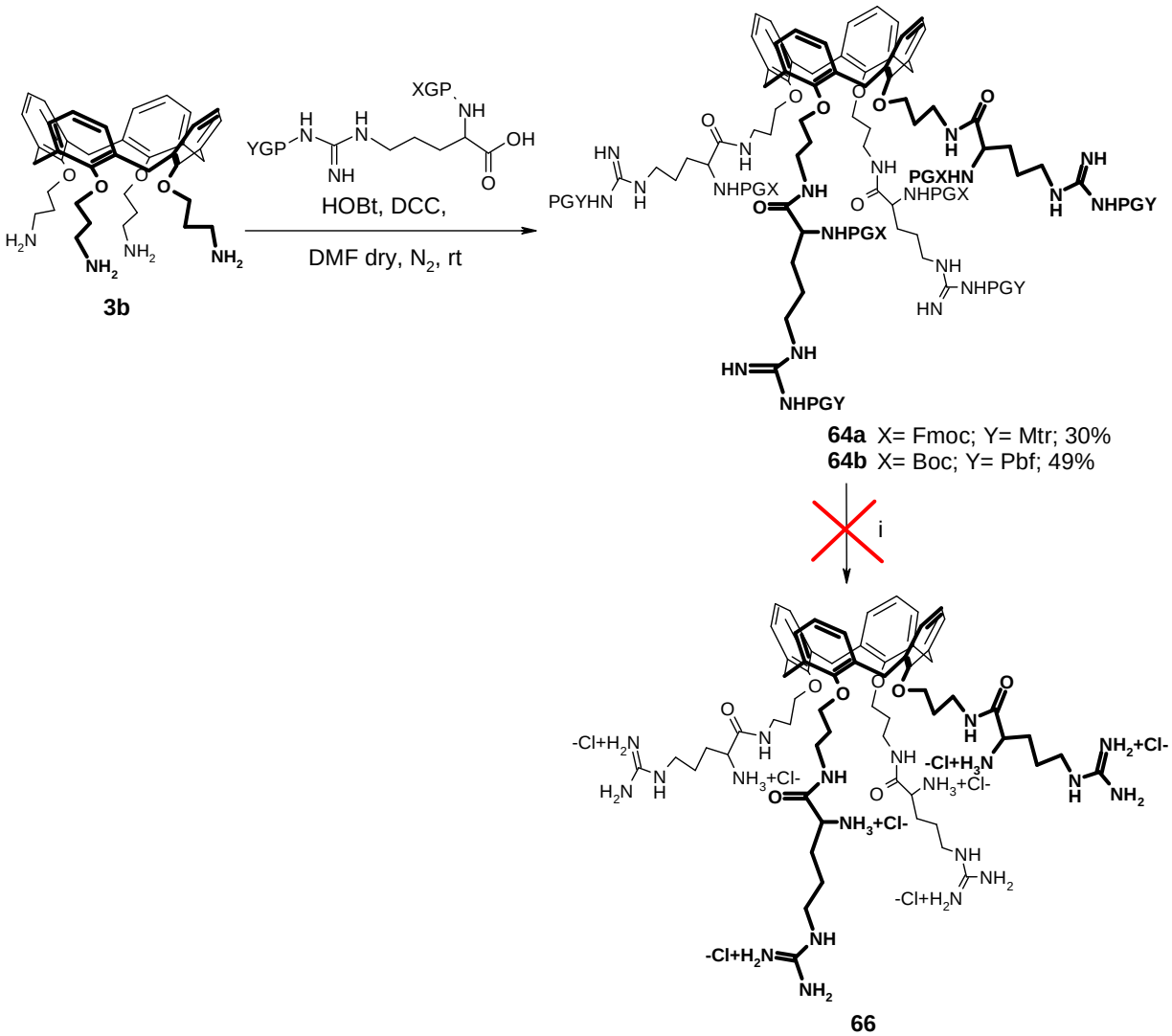

Scheme 4.3. Synthesis of compound **66**. i) 1a) piperidine, dry DCM, N_2, rt; 2a) TFA, TIS, H_2O, dil HCl, rt; 1b) TFA, TIS, H_2O, dil HCl, rt.

Initially, the Fmoc-Arg(Mtr)-OH was used because available in the laboratory, hoping that the difficulties encountered with these protective groups in the synthesis of the upper rim derivative **59**, which we mainly attributed to the structural features of the substrates, would not occur in this case. The coupling product **64a** was isolated not in a very good yield, for the already mentioned problems, and checked by ^{1}H NMR and ESI-MS. Then, the Fmoc groups, in **64a**, were removed as described before, following the reaction by ESI-MS, to get **65**.

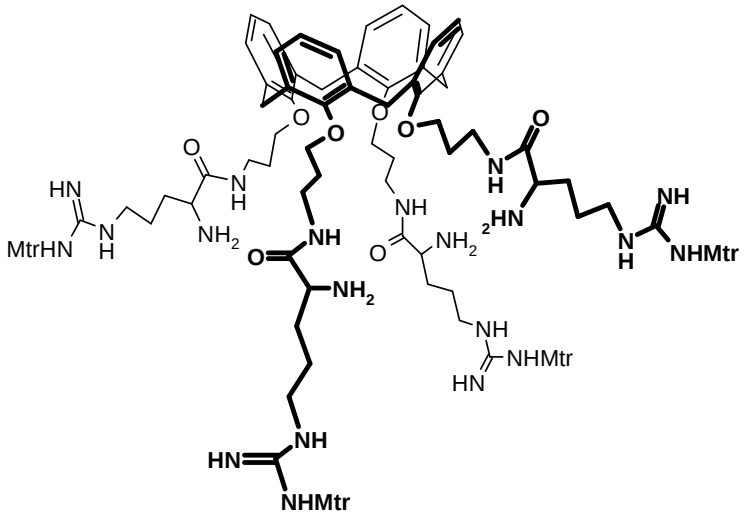

65

The next step was the Mtr deprotection, which resulted very problematic. After the deprotection under the previously described acidic conditions, the ^{1}H NMR spectrum of the reaction product (**Fig. 4.19**) resulted quite complicate, due to the presence of many compounds, clearly evidenced, for instance, by the signals in the aromatic area. Analysis by ESI-MS (**Fig. 4.20**) was also performed and the most significant peak at m/z 638.6 was tentatively assigned to the molecular ion $[M + 3H]^{3+}$ of the partially deprotected product, still bearing one Mtr group. However this signal did not obey to the typical isotopic pattern of a three charged ion. Moreover, the simplicity of the mass spectrum was in contradiction with the complexity of the ^{1}H NMR spectrum (**Fig. 4.19**).

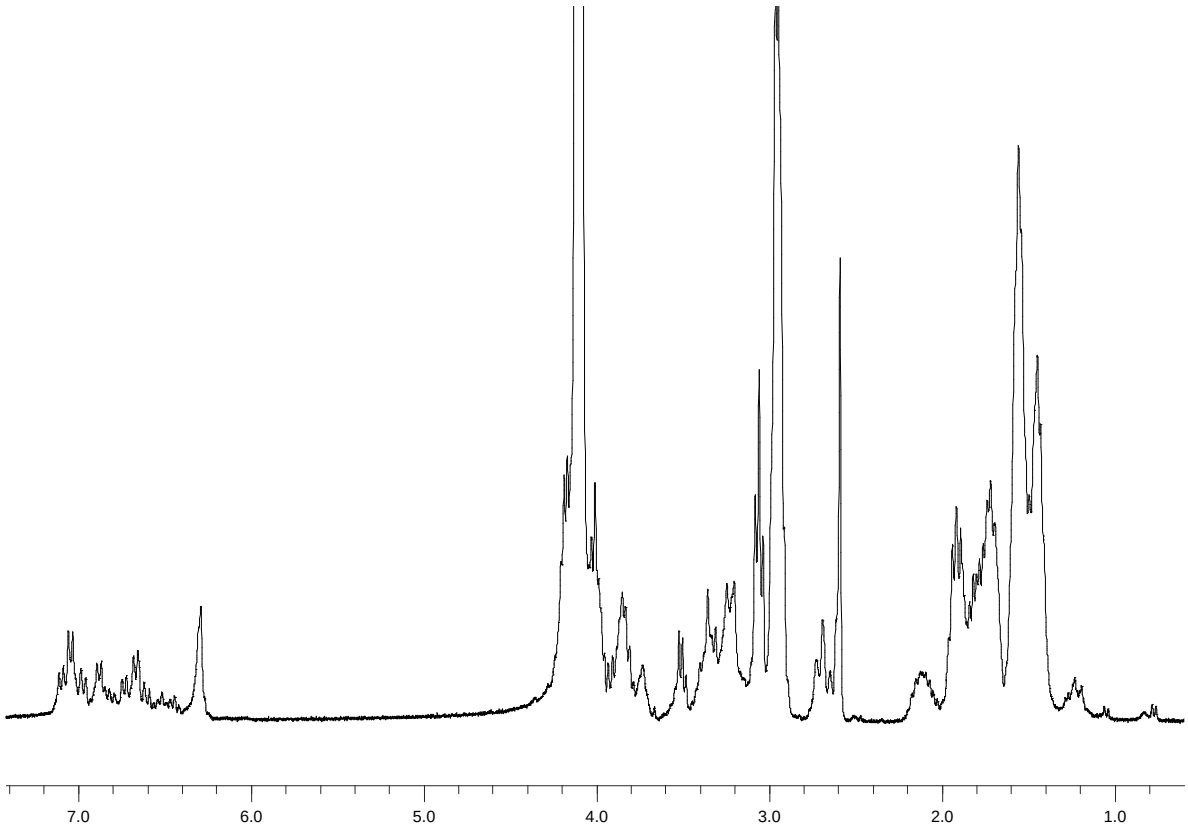

Fig. 4.19. ^{1}H NMR spectrum (CD_3OD, 300 MHz, 298 K) of the crude reaction product **66**, from the deprotection of **65**.

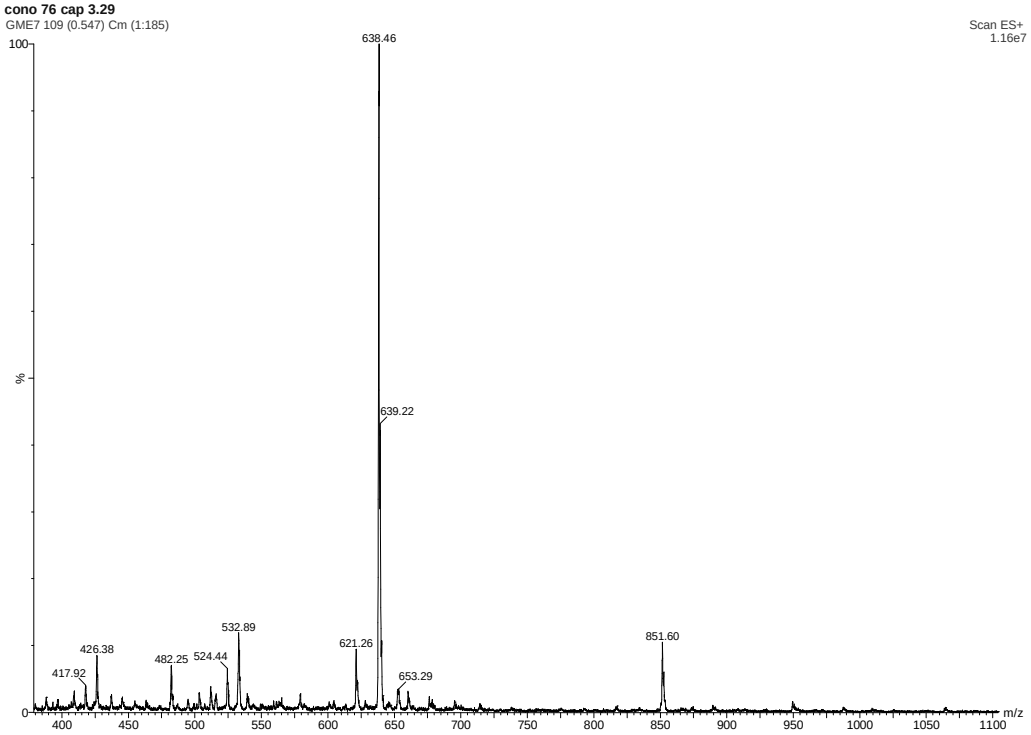

Fig. 4.20. ESI-MS spectrum of the crude reaction product **66**, from deprotection of **65**.

To solve this problem, the reaction was repeated varying times and conditions, but obtaining the same results. So the strategy was changed and as for **59** and **63** we newly resorted to Boc-Arg(Pbf)-OH to obtain compound **64b** (^{1}H NMR in **Fig. 4.21**).

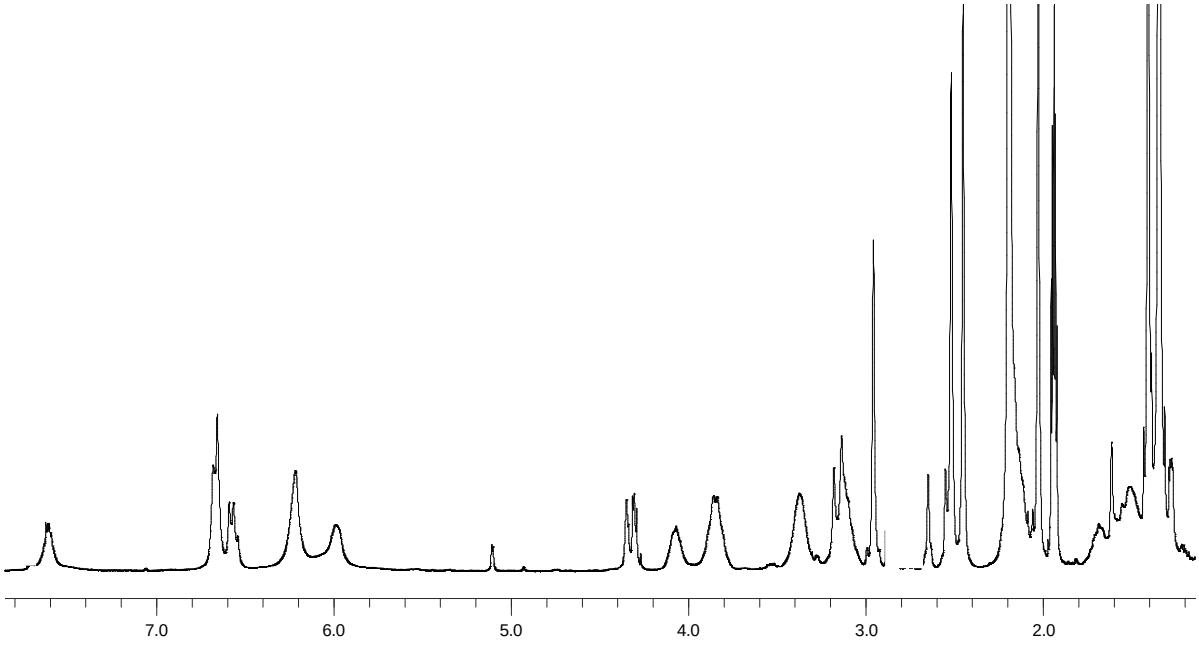

Fig. 4.21. ^{1}H NMR spectrum (CD_3CN, 300 MHz, 298 K) of the compound **64b**.

Unfortunately, after the deprotection reaction, both the ^{1}H NMR (**Fig. 4.22**) and the mass spectra gave results comparable to those observed for **64a**.

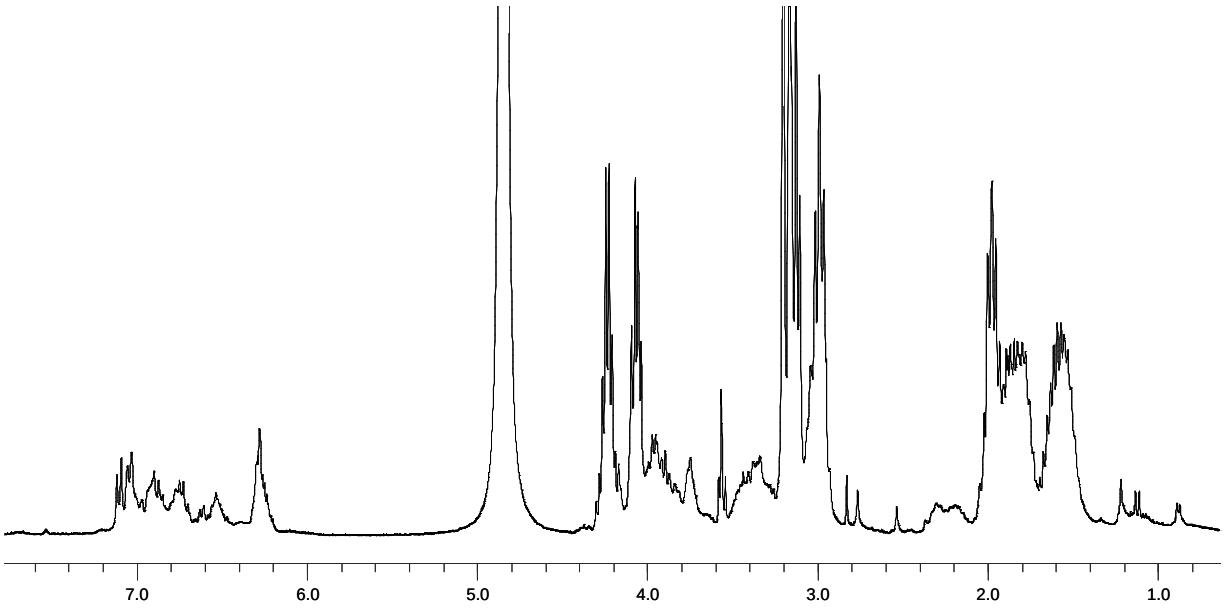

Fig. 4.22. ^{1}H NMR spectrum (CD_3OD, 300 MHz, 298 K) of the crude reaction product, from deprotection of **64b**.

The ^{1}H NMR spectra of the crude reaction products from deprotection of **64a** and **64b** appear very similar (**Fig. 4.19** and **4.22**) and the major peak in the mass spectrum obtained from **64b** is again at m/z 638.5 as observed for the crude product relative to **64a**. These data ruled out our previous conclusion that the compound isolated in the reaction to obtain **64a** was a partially deprotected Mtr derivative, since in **64b** no Mtr protective group is present. A useful information for advancing a reasonable hypothesis on the nature of these unknown compounds derived from deprotection of **64a** and **64b** was obtained performing the deprotection with shorter reaction times. In this case the mass spectrum of the reaction mixture showed, beside the usual peak at m/z 638.5, two other peaks at m/z 851.6 and m/z 1064.7. The mass difference between these two peaks is 213 uma, which correspond to the fragment $Arg(CH_2)_3$. So the three signals could be assigned to calix[4]arenes which have lost three, two or one chain respectively, at the lower rim. This could happen for structural reasons, because at the lower rim the calix[4]arene has four phenolic oxygens, to which the propylarginine chains are linked, that are capable to bind the H_3O^+ ion. This could determine a particular reactivity of H_3O^+, able to justify the ethereal bond cleavage which leads to chain detachment and formation of free phenolic OH groups.[49]

Because the acidic conditions seemed incompatible for the arginine deprotection at the lower rim of the calixarene scaffold, it was thought to use Cbz as protecting group for the alfa amino group, which is removable by hydrogenation. So first the Cbz-Arg-OH was coupled to **3b** (**Scheme 4.4**), monitoring the reaction by a reverse phase TLC. The excess of the protected zwitterionic arginine was removed by silica cartridges, functionalized with ammonium groups. From the ^{1}H NMR spectrum and ESI-MS the reaction resulted to be complete, but some characteristic impurities from the coupling reaction described before were still present.

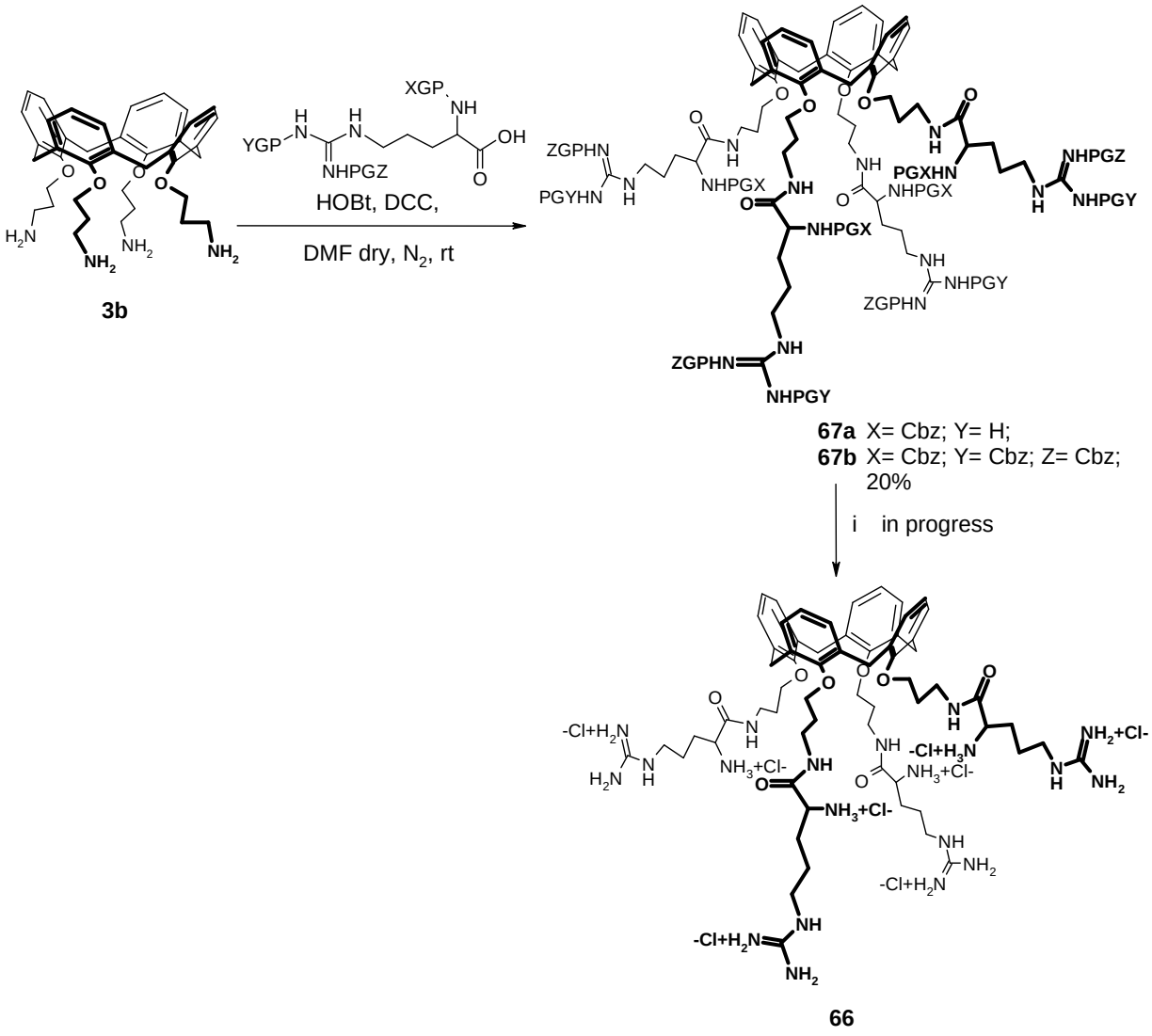

Scheme 4.4. Synthesis of compound **66**. i) Pd/C, MeOH, 2 bar, dil HCl and MeOH, rt; 1b) Pd/C, ethyl acetate, MeOH, rt.

Deprotection of the product by hydrogenation at 2 atm in methanol, in presence of Pd/C, followed by an acid wash with diluted HCl and methanol, to protonate the amino groups, gave compound **66** which, however, could not be isolated in a pure form as verified by ESI-MS and ^{1}H NMR (**Fig. 4.23**).

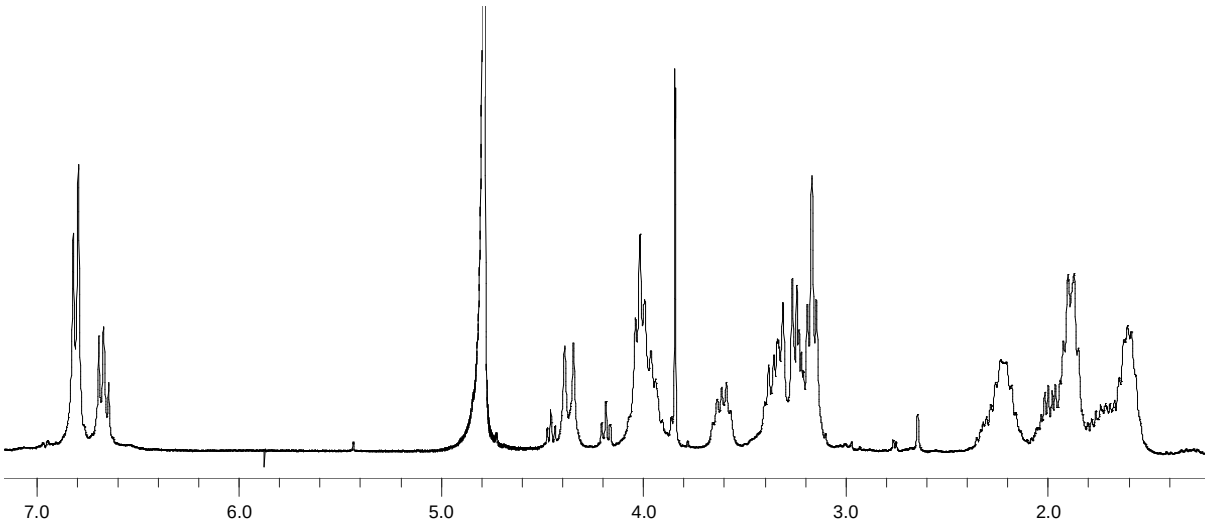

Fig. 4.23. ^{1}H NMR spectrum (D_2O, 300 MHz, 298 K) of the crude reaction product **66**.

New attempts for the purification of compound **66** and for identifying a better method for its synthesis are currently in progress. In particular the deprotection of the fully Cbz protected derivative **67b** is under investigation.

4.2.3 Synthesis of a lower rim arginine-Gemini conjugate

Due to the difficulties encountered in the synthesis of lower rim arginine-calix[4]arene conjugates, the synthesis of the simpler Gemini-type analogue **69** (**Fig. 4.24** and **Scheme 4.5**) was undertaken.

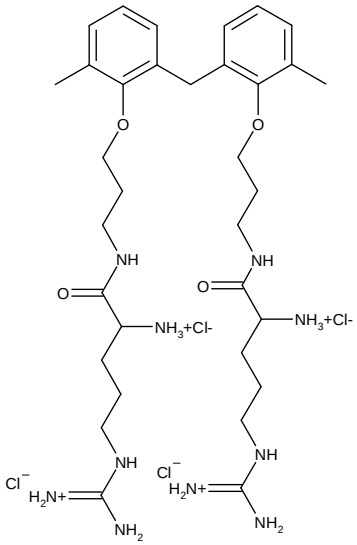

69

Fig. 4.24. Structural formula of the Gemini **69**.

The scope was double, to understand if the previous problems were strictly related to the calixarene structure, and to have once again a linear ligand to confirm a possible macrocyclic effect in interaction with and delivery of DNA. The first step (**Scheme 4.5**) was the usual coupling reaction, in this case between the primary amine **12b** and the Boc-Arg(Pbf)-OH, in presence of HOBt and DCC, obtaining product **68**, that was deprotected with TFA. The latter step was monitored by ESI-MS which after 2 h showed only the peak of the product. The final compound **69** was obtained exchanging the TFA-counterion adding a 10 mM HCl solution and evaporating under reduced pressure.

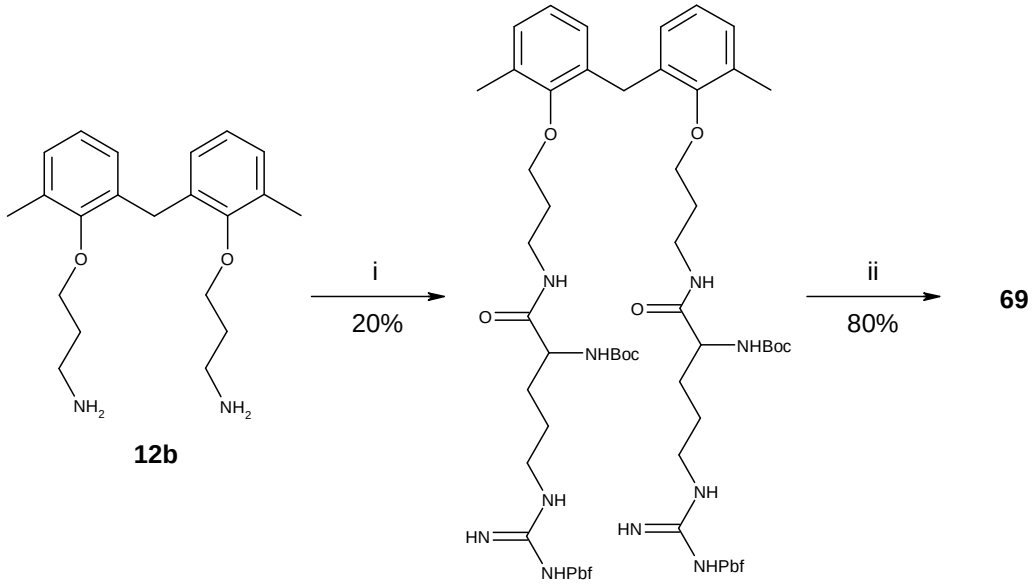

Scheme 4.5. Synthesis of **69**. i) Boc-Arg(Pbf)-OH, HOBt, DCC, dry DMF, N_2, rt; ii) TFA, TIS, H_2O, dil HCl, rt.

In the ^{1}H NMR and ^{13}C NMR spectra registered in CD_3OD all the peaks relative to the protecting groups are absent. The easy synthesis of **69** showed that the breaking of the propylargininamido chains occurs for the calixarene because of some specific structural features which, as mentioned above, could be related with a particular proximity of H_3O^+ ion to the phenolic oxygen atoms.

4.2.4 NMR spectra of arginine conjugates in D_2O

The three arginino-derivatives **59**, **63** and **69** succesfully synthesized were studied in D_2O at different concentrations.

Arginino-calixarene **59** is poorly soluble in water and ^{1}H NMR spectra in D_2O evidence broad signals (**Fig. 4.25**) suggesting marked aggregation phenomena due to the alkyl chains at the lower rim, even at concentrations close to the detection limit of the technique.

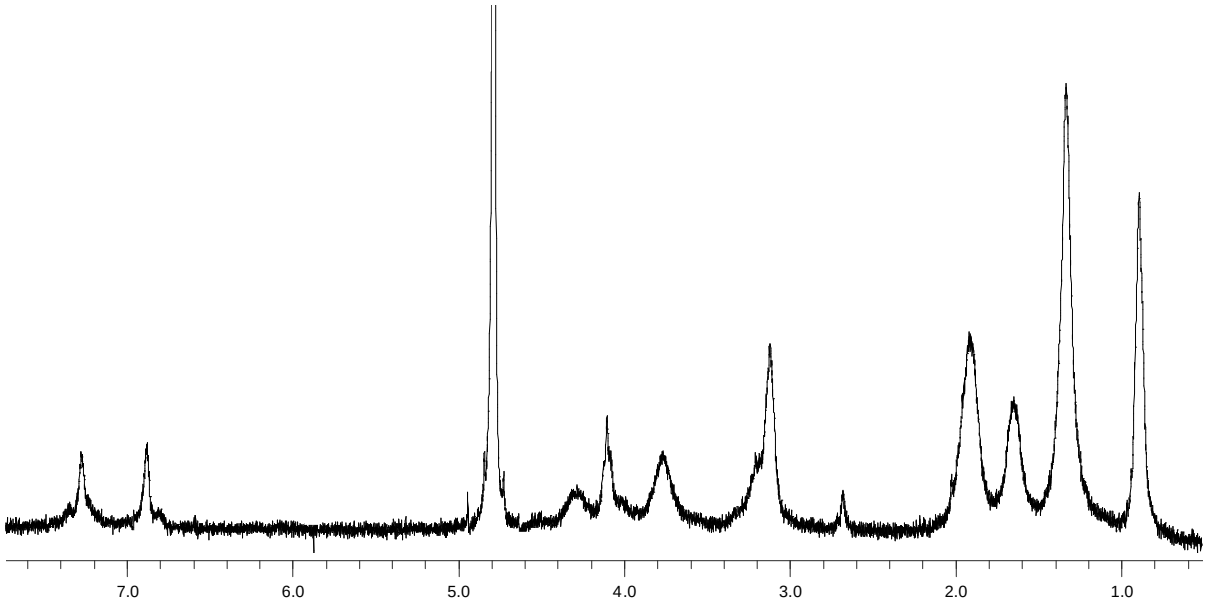

Fig. 4.25. ^{1}H NMR spectrum (D_2O, 300 MHz, 298 K) of compound **59**.

Its analogue **63** with ethoxyethyl chains resulted more soluble in D_2O, showing on the contrary narrow signals in the spectrum indicating that aggregation does not occur (**Fig. 4.26**) at mM concentrations where NMR experiments were registered.

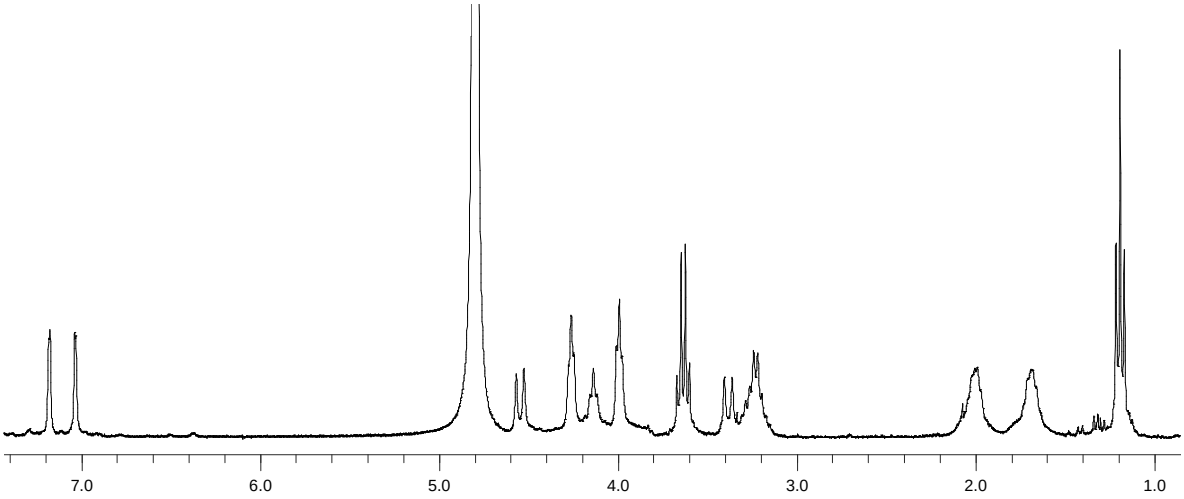

Fig. 4.26. ^{1}H NMR spectrum (D_2O, 300 MHz, 298 K) of compound **63**.

The lower rim arginino-Gemini is soluble in D_2O and it shows narrow signals very well resolved (**Fig. 4.27**) for each proton.

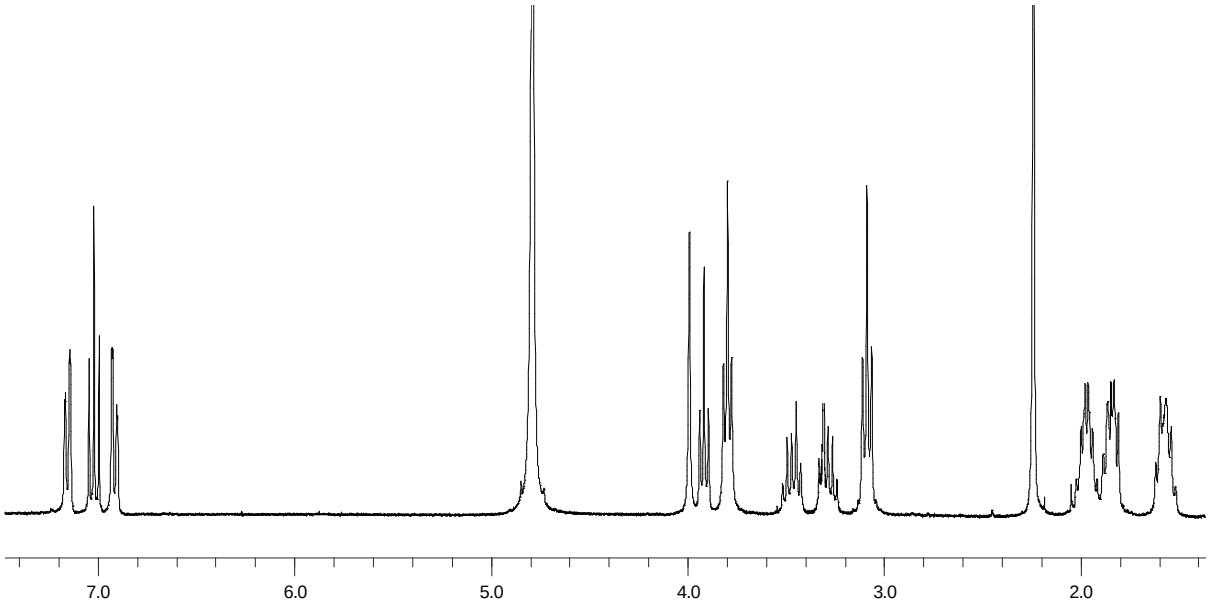

Fig. 4.27. Spectrum ^{1}H NMR (D_2O, 300 MHz, 298 K) of **69**.

4.2.5 DNA binding and cell transfection

The capacity to bind DNA was studied by EMSA (**Fig. 4.28**) for compound **59**, which clearly interacts already at 50 μM and it keeps the plasmid totally in the well at a concentration of 100 μM

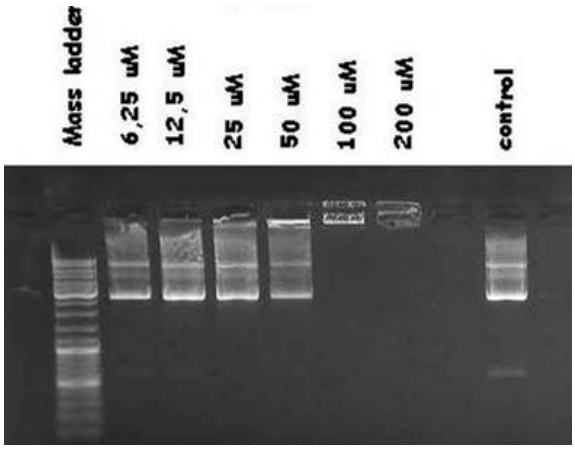

Fig. 4.28. Electrophoresis mobility shift assay performed with plasmid DNA (pEGFP-C1) (25 nM) incubated with calix[4]arene **59** at increasing concentrations (indicated above the gel). The control is plasmid without ligand.

The interaction was then studied by AFM and the recorded images (**Fig. 4.29**) show the capacity of calix[4]arene **59** to strongly modify the plasmid DNA, forming at 1 μM ligand of one or more filaments. The decrease in the concentration to 0.5 μM leads to the formation of some smaller condensates, while part of the filaments visible on the surface appear in almost relaxed form (**Fig. 4.29c**). Actually, on the basis of collected AFM data, compared to other

our ligands, **59** did not show the best performance in giving rise to small condensates, considered by us the best ones in the perspective of gene delivery.

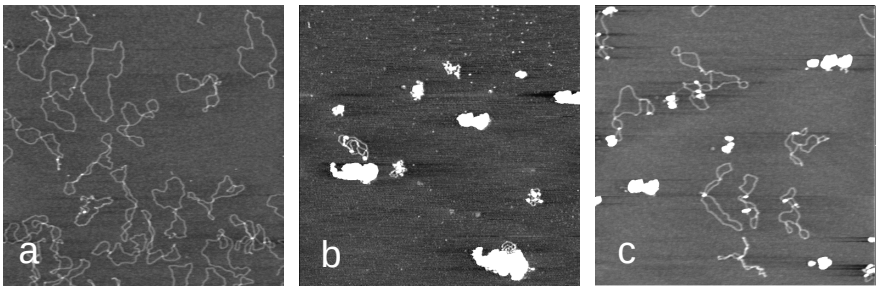

Fig. 4.29. AFM images showing the effects induced on plasmid DNA by **59**. All images were obtained with the microscope operating in tapping mode in air and with supercoiled pEGFP-C1 plasmid deposited onto mica at a concentration of 1 nM. a) Plasmid alone. Plasmid incubated with b) **59** 1 μM and c) **59** 0.5 μM. Each image represents a 2×2 μm scan.

The AFM images of **63** show a very different behaviour compared to **59**. Interactions occur without doubt both in presence and in absence of ethanol. In the concentration range between 10^{-6} to 10^{-5} M, and at 1-2.5 μM (**Fig. 4.30a-b**) some big aggregates constituted by multiple filaments are present. Adding a small percentage of ethanol the situation does not really change (**Fig. 4.30c**). All together these data indicate a scarce propensity of compound **63**, having more hydrophilic tails, to condense efficiently single filaments of DNA, pointing out the importance of hydrophobic alkyl chains at the lower rim of calix[4]arenes promoting DNA condensation.

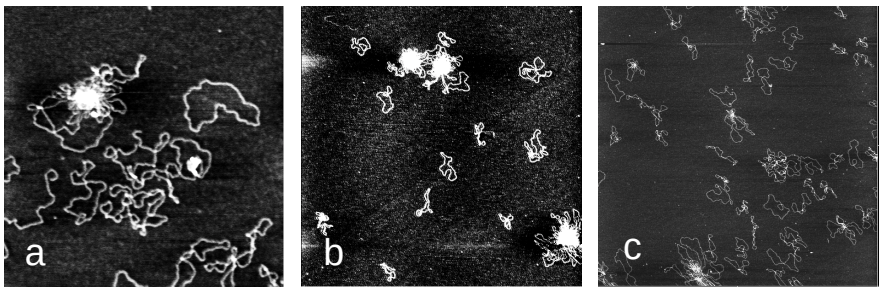

Fig. 4.30. AFM images showing the effects induced on plasmid DNA by **63**. All images were obtained with the microscope operating in tapping mode in air and with supercoiled pEGFP-C1 plasmid deposited onto mica at a concentration of 1 nM. Plasmid incubated with a) **63** 1 μM, b) **63** 2.5 μM and c) **63** 1 μM + 5% EtOH. The first image is a 2×2 μm scan, the second and the third a 5×5 μm scan.

The Gemini **69** is not active in the condensation of the plasmid, at different concentrations and (from 10^{-6} to 10^{-5} M) in absence or in presence of EtOH (10% V/V). The AFM images (**Fig. 4.31**) showed plasmids modified in their shape compared to their relaxed form, but even at 10^{-5} M no real condensates were observed.

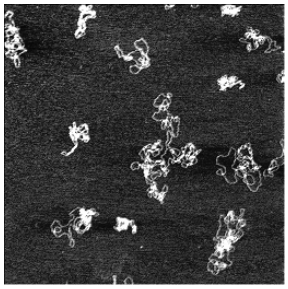

Fig. 4.31. AFM image (2×2 μm) of plasmid 0.5 nM in presence of **69** 5×10^{-5} M.

The usual transfection experiments (see **Chapters 2**, **3**) were then performed, in absence and in presence of DOPE, for all the compounds obtained in the pure form.

In the same transfection conditions of the lower rim guanidinium calixarenes (see **Chapters 2**, **3**), **59** resulted much more efficient in transfecting the rhabdomyosarcoma cell line. Also in absence of DOPE, it is able to transfect more then 90% of the cells, even if a longer time is needed to reach this high percentage (**Fig. 4.32**). Quite interestingly, a negligible cytotoxicity characterizes the action of this ligand.

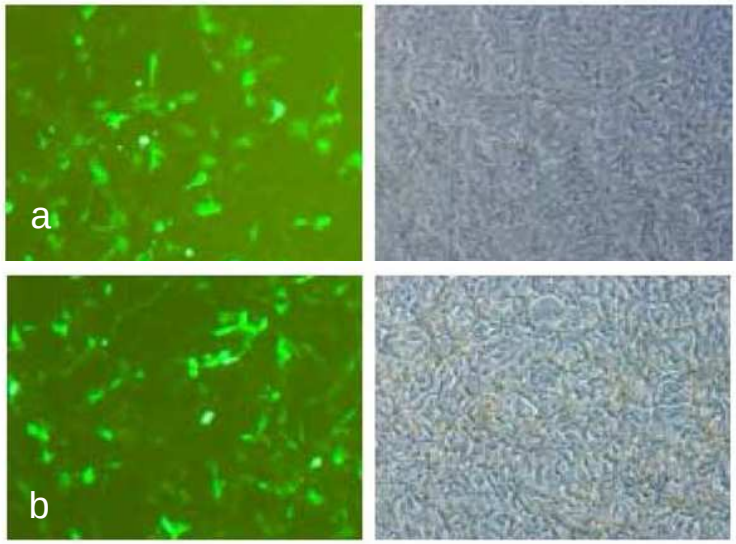

Fig. 4.32. Transfection experiments performed with pEGFP-C1 plasmid 1 nM and a) ligand **59** 10 μM and b) **59**/DOPE (10/20 μM), to rhabdomyosarcoma cells. Images are obtained by fluorescence microscopy (on the left) and by phase contrast microscopy (on the right).

Hoping that the fluorescent calixarene **55** could be involved in the very efficient delivery process driven by **59**, the peptidocalixarene, the best transfecting calixarene found up to now, was also mixed with the coumarin bearing ligand. Used in the ratio of 4/1, this mixture was incubated with the plasmid DNA and the cells. The transfection worked again with efficiency (**Fig. 4.33**), thanks evidently to the presence of **59** whose properties are not negatively affected by the presence of **55**, but blue fluorescence was not observed. As noticed in similar

experiments with **5b**, the quenching of fluorescence or the complete exclusion of the fluorophore-calixarene conjugate from transfection, nullified the idea of following the fate of the vector inside the cells.

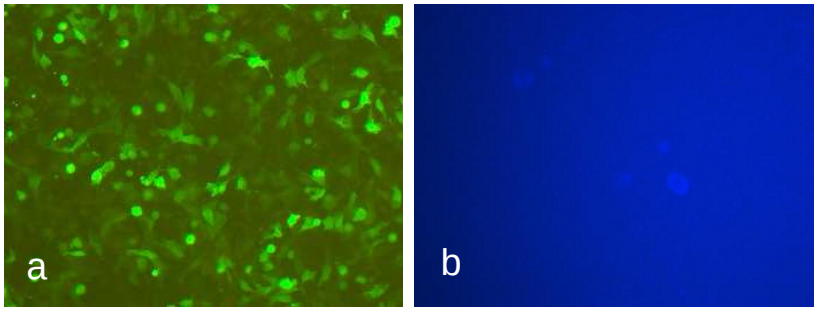

Fig. 4.33. Transfection experiments performed with a mixture of vector **59** and ligand **48** collecting a) in the green, where the green fluorescent protein emits, b) in the blue, where **48** emits. Cells are visualized with fluorescence microscopy.

4.3 Discussion and Conclusions

The studies aimed at the conjugation of arginine units to a calix[4]arene platform and described in this chapter revealed some pitfalls but also some quite interesting features. Unespected synthetic difficulties, which are not present in the functionalisation of linear scaffold such as **12b**, which smoothly gives the Gemini-type arginino derivative **69**, were encountered in the functionalisation of calix[4]arenes with arginine moieties, especially at the lower rim. The conjugation of protected arginines, both at amino and guanidine groups, occurred rather easily and the difficulties were encountered especially in the deprotection steps. It has been evidenced that the strongly acidic conditions used to remove the Tosyl and the Mtr protective groups are not particularly compatible with the calix[4]arene derivatives, leading to substantial cleavage of amide bonds at the upper or ethereal bonds at the lower rim. Evidence has been collected that, especially for the lower rim, complexation of H_3O^+ cation enhances its catalytic reactivity towards the scissible bonds. These results are in agreement with previously reported examples of calixarene arginine conjugates, where a very long and difficult deprotection procedure was used.[41] In spite of these synthetic difficulties two upper rim arginine-calix[4]arene conjugates **59** and **63** have been synthesized as pure compounds, whereas the lower rim analogue of guanidinium calix[4]arene **5b** has been obtained in mixture with other by-products.

We were pleased to see that compound **59**, bearing four arginine moieties at the upper rim, is able to transfect cells quite efficiently, showing also very little toxicity. As a matter of fact **59** is the most effective calixarene-based vector synthesized so far. This compound is able to transfect cells even in the absence of helper lipids, such as DOPE. The AFM and EMSA

studies reveal that compound **59** interacts with plasmid DNA and condenses it in "blobs" of suitable size to be internalized in the cell, even if from both type of experiments it did not appear as the best one, if compared for example with **5a-c** guanidinium calixarenes. On the other hand, compound **63**, which is very similar to **59** but has four, more hydrophilic ethoxyethyl chains at the lower rim instead of hexyl groups as in **59**, does not condense efficiently DNA filaments and it is in fact a poor transfectant. This observation points out the importance of hydrophobic interactions in determining the DNA condensation and transfection properties in this class of vectors.

Also in this case, as observed for simple guanidinium derivatives (see **Chapter 2**) the Gemini-arginino derivative **69** is not able to condense DNA, even in presence of ethanol, and does not transfect cells. Although compound **69**, which bears the arginine moiety at the lower rim, cannot be strictly compared with upper rim arginino-calix[4]arenes **59** and **63**, these results strengthen the idea that macrocyclic vectors are more efficient than linear analogues in DNA condensation and cell transfection.

In conclusion, the lead compound **59** four important features are present, which could explain its remarkable properties:

1) it is a macrocyclic vector;
2) it possesses four hexyl chains at the lower rim which, after the first electrostatic interactions of the charged cationic groups with the DNA phosphate backbone, hydrophobically interact between them facilitating the condensation of single DNA filaments as observed previously for upper rim guanidinium calixarenes;[50]
3) in addition to guanidinium groups, **59** has four primary ammonium groups which can eventually interact with the phosphate residues both of the DNA double helix and cell membrane phospholipids, enhancing the binding and cell penetration ability of the lipoplex. Moreover, the protonation state of these ammonium groups is pH dependent and it could be ruled out that inside the cell, some of these groups might not be protonated and the DNA filaments could be released intact through the "proton sponge" effect outlined in the **Introduction**;
4) finally, compound **59** is characterised by the presence of four amide bonds which could be cleaved by enzymes inside the cell helping the release of nucleic acid and biodegradation of the vector. This last effect could also explain the very low toxicity shown by this vector and specific studies will be carried out in order to ascertain its existence.

The fact that compound **59** is able to perform transfection alone without the addition of an helper lipid, as usually done with commercial formulation used in cell transfection, and its very low toxicity are very attractive features for using this molecule in gene therapy.

4.4 Experimental section

All the reactions were carried out under a nitrogen atmosphere. All dry solvents were prepared according to standard procedures and stored over molecular sieves. Melting points were determined on an Electrothermal apparatus in capillaries sealed under nitrogen. ^{1}H and ^{13}C NMR spectra were recorded on Bruker AV300 and AC300 spectrometers (partially deuterated solvents were used as internal standards). Mass spectra were recorded in ESI mode on a single quadrupole instrument SQ Detector, Waters (capillary voltage 3.8 kV, cone voltage 30-160 eV, extractor voltage 3 eV, source block temperature 80 °C, desolvation temperature 150 °C, cone and desolvation gas (N_2) flow rates 1.6 and 8 L/min, respectively). TLC was performed on Merck 60 F254 silica gel and flash column chromatography on 230-240 mesh Merck 60 silica gel.

Synthesis of 5,11,17,23-Tetranitro-25,26,27,28-tetrakis(ethoxyethoxy)calix[4]arene (60).
It was obtained starting from the t-butyl analogue,[48] via standard ipsonitration for calixarenes.[51] The crude material was purified by column chromatography (eluent: cyclohexane/ethyl acetate= 2:3) to obtain the pure product as a white solid in 20% yield.
Mp: 180-183 °C. ^{1}H NMR (300 MHz, $CDCl_3$) δ 7.56 (s, 8H, Ar*H*), 4.67 (d, *J* = 14.0 Hz, 4H, ArC*H*$_2$Ar), 4.23 (t, *J* = 4.6 Hz, 8H, ArOC*H*$_2$), 3.77 (t, *J* = 4.6 Hz, 8H, ArOCH$_2$C*H*$_2$), 3.48 (q, *J* = 6.9 Hz, 8H, ArOCH$_2$CH$_2$OC*H*$_2$), 3.36 (d, *J* = 14.0 Hz, 4H, ArC*H*$_2$Ar), 1.15 (t, *J* = 6.9 Hz, 12H, C*H*$_3$). ^{13}C NMR (75 MHz, $CDCl_3$) δ 161.7, 142.8, 135.6, 123.8, 74.4, 69.4, 66.4, 30.9, 15.1. MS (ESI): calculated for $[M + Na]^+$ *m/z* = 915.3, found *m/z* = 915.0.

Synthesis of 5,11,17,23-Tetramino-25,26,27,28-tetrakis(*n*-hexyloxy)calix[4]arene (61).
It was synthesized according to a literature procedure.[50]
The pure product was obtained as a red solid in 42% yield.
Mp: 137 °C dec. ^{1}H NMR (300 MHz, $CDCl_3$) δ 6.06 (s, 8H, Ar*H*), 4.33 (d, *J* = 13.2 Hz, 4H, ArC*H*$_2$Ar), 4.08-3.65 (m, 16H, ArOC*H*$_2$C*H*$_2$), 3.65-3.40 (m, 8H, ArOCH$_2$CH$_2$OC*H*$_2$), 3.22-2.72 (m, 12H, ArC*H*$_2$Ar and ArN*H*$_2$), 1.34-1.04 (m, 12H, C*H*$_3$). ^{13}C NMR (75 MHz, $CDCl_3$) δ

149.7, 140.5, 135.4, 115.6, 73.0, 69.5, 66.3, 30.9, 15.2. MS (ESI): calculated for $[M + 2Na]^{++}$ *m/z* = 795.4, found *m/z* = 795.2.

Synthesis of 25,26,27,28-Tetrakis(3-aminopropoxy)calix[4]arene (56).

It was synthesized according to a literature procedure.[52]

General procedure for the synthesis of arginine protected derivatives (procedure similar to ref. 54). To a stirring DMF solution (2 mL) of protected arginine derivative (6 eq.), HOBt (6.8 eq.) and DCC (6 eq.) were added. After 15 min, a solution of calix[4]arene or linear compound (0.15 mmol) (1 eq.) in 2 mL of DMF was dropped. The mixture was stirred at rt for 24 h. Ethyl acetate was added (10 mL), DCU was filtered off on a Hirsch funnel, the organic layer was washed with a saturated $NaHCO_3$ aqueous solution (5 mL), brine (3×10 mL) and dried over anhydrous Na_2SO_4. The solvent was removed under reduced pressure giving a crude material which was purified as indicated below.

5,11,17,23-Tetrakis[(Nα-Boc-Nω–Tos-L-Arg)amino]-25,26,27,28-tetrakis(*n*-hexyloxy)calix[4]arene (57a).

The crude material was purified by preparative TLC (eluent: CH_2Cl_2/MeOH= 94:6) to obtain the pure product as a white solid in 15% yield.

^{1}H NMR (300 MHz, CD_3OD) δ 7.71 (d, *J* = 7.9 Hz, 8H, Tos), 7.23 (d, *J* = 7.9 Hz, 8H, Tos), 7.03 (bs, 4H, Ar*H*), 6.72 (bs, 4H, Ar*H*), 4.47 (d, *J* = 13.0 Hz, 4H, ArCH_2Ar), 4.10 (bs, 4H, COC*H*NH), 3.91 (t, *J* = 6.9 Hz, 8H, ArOCH_2), 3.18 (bs, 8H, CH_2NH), 3.13 (d, *J* = 13.0 Hz, 4H, ArCH_2Ar), 2.32 (s, 12H, CH_3Tos), 2.00-1.88 (m, 8H, OCH_2CH_2), 1.80-1.25 (m, 76H, $OCH_2CH_2CH_2CH_2CH_2$, $CH_2CH_2CH_2NH$ and *t*Bu), 0.96 (t, *J* = 6.7 Hz, 12H, CH_2CH_3). ^{13}C NMR (75 MHz, CD_3OD) δ 173.1, 160.4, 159.9, 155.1, 143.8, 142.4, 136.6, 133.5, 130.6, 127.4, 123.1, 122.2, 81.1, 76.8, 56.4, 40.1, 33.7, 32.5, 31.7, 31.2, 29.2, 27.6, 24.3, 21.7, 14.8. MS (ESI): calculated for $[M + 2Na]^{++}$ *m/z* = 1253.6, found *m/z* = 1254.2.

5,11,17,23-Tetrakis[(Nα-Fmoc-Nω–Mtr-L-Arg)amino]-25,26,27,28-tetrakis(*n*-hexyloxy)calix[4]arene (57b).

The crude material was purified by column chromatography (eluent: ethyl acetate/hexane= 4:1) to obtain the pure product as a white solid in 17% yield.

Mp: 160-162 °C. ^{1}H NMR (300 MHz, CD_3Cl_3/CD_3OD= 19:1) δ 8.97 (bs, 4H, ArN*H*), 7.66 (d, *J* = 7.1 Hz, 8H, ArFmoc), 7.48 (d, *J* = 5.4 Hz, 8H, ArFmoc), 7.30 (t, *J* = 7.1 Hz, 8H,

ArFmoc), 7.25-7.10 (m, 8H, ArFmoc), 6.96 (bs, 4H, Ar*H*), 6.42 (bs, 8H, Ar*H* and ArMtr), 4.40 (d, *J* = 12.4 Hz, 4H, ArCH_2Ar), 4.35-4.10 (m, 12H, CH_2C*H*Fmoc), 4.10-4.00 (m, 4H, COC*H*NH), 3.84 (bs, 8H, ArOCH_2), 3.69 (s, 12H, OCH_3Mtr), 3.30-3.00 (m, 12H, ArCH_2Ar and CH_2NH), 2.62 (s, 12H, CH_3Mtr), 2.56 (s, 12H, CH_3Mtr), 2.02 (s, 12H, CH_3Mtr), 1.91 (bs, 8H, OCH$_2$CH_2), 1.85-1.25 (m, 40H, OCH$_2$CH$_2$CH_2CH_2CH_2 and CH_2CH_2CH$_2$NH), 0.95-0.83 (m, 12H, CH$_2$CH_3). ^{13}C NMR (75 MHz, CD_3Cl_3/CD_3OD= 19:1) δ 170.8, 158.4, 156.5, 156.4, 153.6, 143.7, 143.5, 141.1, 138.4, 136.4, 135.1, 133.0, 127.6, 127.0, 125.0, 124.8, 121.5, 119.8, 111.7, 75.5, 66.9, 55.3, 55.0, 46.9, 39.8, 32.0, 31.0, 30.0, 29.6, 25.8, 25.3, 24.0, 22.7, 18.3, 14.0, 11.8. MS (ESI): calculated for [M + 2Na]$^{++}$ *m/z* = 1613.7, found *m/z* = 1614.5.

5,11,17,23-Tetrakis[(Nα-Boc-Nω–Pbf-L-Arg)amino]-25,26,27,28-tetrakis(*n*-hexyloxy)calix[4]arene (57c).

The crude material was purified by preparative TLC (eluent: CH_2Cl_2/MeOH= 96:4) to obtain the pure product as a white solid in 20% yield.

Mp: 156-158 °C. ^{1}H NMR (300 MHz, CD_3Cl_3/CD_3OD= 19:1) δ 9.04 (bs, 4H, ArN*H*), 7.10-6.10 (bs, 8H, Ar*H* and N*H*CN*H*N*H*), 5.90 (bs, N*H*Boc), 4.33 (d, *J* = 13.1 Hz, 4H, ArCH_2Ar), 4.06 (bs, 4H, COC*H*NH), 3.77 (bs, 8H, OCH_2), 3.10 (bs, 8H, CH_2NH), 3.04 (d, *J* = 13.1 Hz, 4H, ArCH_2Ar), 2.89 (s, 8H, CH_2Pbf), 2.49 (s, 12H, CH_3Pbf), 2.43 (s, 12H, CH_3Pbf), 2.00 (s, 12H, CH_3Pbf), 1.90-1.20 (m, 108H, OCH$_2$CH_2CH_2CH_2CH_2, *t*Bu and C(CH_3)$_2$Pbf), 0.84 (t, *J* = 6.5 Hz, 12H, CH$_2$CH_3). ^{13}C NMR (75 MHz, CD_3Cl_3/CD_3OD= 19:1) δ 171.0, 158.6, 156.3, 155.9, 153.5, 138.2, 134.9, 132.4, 132.2, 131.0, 124.6, 121.0, 117.4, 86.4, 79.9, 75.3, 54.3, 43.0, 40.2, 31.9, 31.0, 30.0, 29.6, 28.3, 28.1, 25.8, 25.1, 22.7, 19.1, 17.8, 13.9, 12.2. MS (ESI): calculated for [M + 2Na]$^{++}$ *m/z* = 1449.8, found *m/z* = 1450.6.

5,11,17,23-Tetrakis[(Nα-Boc-Nω–Pbf-L-Arg)amino]-25,26,27,28-tetrakis(ethoxyethoxy)calix[4]arene (62).

The crude material was purified by preparative TLC (eluent: ethyl acetate/EtOH= 98:2) to obtain the pure product as a white solid in 10% yield.

Mp: 190-193 °C. ^{1}H NMR (300 MHz, CD_3Cl_3/CD_3OD= 19:1) δ 9.05 (bs, 4H, ArN*H*), 6.87 (bs, 4H, Ar*H*), 6.63 (bs, 4H, Ar*H*), 4.35 (d, *J* = 13.0 Hz, 4H, ArCH_2Ar), OCH_2 and C*H*CONH under the HOD, 3.70 (bs, 8H, ArOCH_2), 3.50-3.35 (m, 8H, ArOCH$_2$CH_2), 3.15-2.92 (m, 12H, CH_2NH), 3.04 (d, *J* = 13.0 Hz, 4H, ArCH_2Ar), 2.82 (s, 8H, CH_2Pbf), 2.42 (s, 12H, CH_3Pbf), 2.36 (s, 12H, CH_3Pbf), 1.94 (s, 12H, CH_3Pbf), 1.80-1.05 (m, 88H, COCHCH_2CH_2, *t*Bu,

C(C*H*$_3$)$_2$Pbf and CH$_2$C*H*$_3$). ^{13}C NMR (75 MHz, CD$_3$Cl$_3$/CD$_3$OD= 19:1) δ 171.1, 158.8, 155.9, 153.1, 138.4, 134.9, 132.4, 131.4, 124.7, 121.0, 117.5, 86.5, 79.8, 73.0, 69.3, 66.2, 54.2, 42.9, 33.4, 29.4, 28.1, 27.9, 25.3, 24.6, 18.9, 17.6, 14.8, 12.0. MS (ESI): calculated for [M + 2Na]$^{++}$ *m/z* = 1425.7, found *m/z* = 1425.9.

25,26,27,28-Tetrakis{3-[(Nα-Fmoc-Nω–Mtr-L-Arg)amino]propoxy}calix[4]arene (64a).

The crude material was purified by column chromatography (eluent: from CH$_2$Cl$_2$/MeOH= 100:1 to 96:4) to obtain the pure product as a white solid in 30% yield.

Mp: 158-160 °C. ^{1}H NMR (300 MHz, CD$_3$Cl$_3$/CD$_3$OD= 19:1) δ 7.95 (bs, 4H, CH$_2$N*H*CO), 7.65 (d, *J* = 6.6 Hz, 8H, ArFmoc), 7.44 (d, *J* = 6.6 Hz, 8H, ArFmoc), 7.35-7.20 (m, 8H, ArFmoc), 7.15 (t, *J* = 6.6 Hz, 8H, ArFmoc), 6.60-6.10 (m, 24H, Ar*H*, ArMtr, CHN*H*CO and CH$_2$N*H*CNH), 4.42-4.20 (m, 12H, ArC*H*$_2$Ar and OC*H*$_2$CHFmoc), 4.18 (bs, 4H, OCH$_2$C*H*Fmoc), 4.00 (bs, 4H, COC*H*NH), 3.93 (bs, 8H, ArOC*H*$_2$), 3.74 (s, 12H, OC*H*$_3$Mtr), 3.32 (bs, 8H, OCH$_2$CH$_2$C*H*$_2$), 3.17 (bs, 8H, C*H*$_2$NHCN), 3.08 (d, *J* = 13.0 Hz, 4H, ArC*H*$_2$Ar), 2.63 (s, 12H, C*H*$_3$Mtr), 2.57 (s, 12H, C*H*$_3$Mtr), 2.10 (bs, 8H, OCH$_2$C*H*$_2$), 2.05 (s, 12H, C*H*$_3$Mtr), 1.80 (bs, 8H, COCHC*H*$_2$), 1.60 (bs, 8H, COCHCH$_2$C*H*$_2$). ^{13}C NMR (75 MHz, CD$_3$Cl$_3$/CD$_3$OD= 19:1) δ 170.7, 156.2, 154.4, 154.3, 153.7, 141.5, 141.3, 138.9, 136.1, 134.2, 132.5, 130.9, 126.0, 125.4, 124.7, 122.8, 122.6, 120.1, 117.6, 109.5, 70.3, 64.9, 53.1, 52.4, 44.7, 37.8, 35.0, 28.4, 27.9, 27.5, 23.4, 21.9, 16.1, 9.7. MS (ESI): calculated for [M + 2Na]$^{++}$ *m/z* = 1529.6, found *m/z* = 1530.6.

25,26,27,28-Tetrakis{3-[(Nα-Boc-Nω–Pbf-L-Arg)amino]propoxy}calix[4]arene (64b).

The crude material was purified by column chromatography (eluent: from ethyl acetate/hexane= 7:3 to ethyl acetate/MeOH= 98:2) to obtain the pure product as a white solid in 49% yield.

Mp: 162-164 °C. ^{1}H NMR (300 MHz, CD$_3$CN) δ 7.61 (bs, 4H, CH$_2$N*H*CO), 6.66 (d, *J* = 6.9 Hz, 8H, Ar*H*), 6.56 (t, *J* = 6.9 Hz, 4H, Ar*H*), 6.21 (bs, 12H, N*H*CN*H*N*H*), 5.99 (bs, 4H, N*H*Boc), 4.32 (d, *J* = 13.1 Hz, 4H, ArC*H*$_2$Ar), 4.04 (bs, 4H, COC*H*NH), 3.83 (bs, 8H, OC*H*$_2$), 3.36 (bs, 8H, OCH$_2$CH$_2$C*H*$_2$), 3.15 (d, *J* = 13.1, 4H, ArC*H*$_2$Ar), 3.13 (bs, 8H, C*H*$_2$NHCNH), 2.95 (s, 8H, C*H*$_2$Mtr), 2.51 (s, 12H, C*H*$_3$Pbf), 2.44 (s, 12H, C*H*$_3$Pbf), 2.15 (bs, 8H, OCH$_2$C*H*$_2$), 2.02 (s, 12H, C*H*$_3$Pbf), 1.75-1.20 (m, 16H, COCHC*H*$_2$C*H*$_2$CH$_2$NH), 1.40 (s, 24H, C(C*H*$_3$)$_2$Pbf), 1.34 (s, 36H, *t*Bu). ^{13}C NMR (75 MHz, CD$_3$CN) δ 173.8, 158.9, 157.1, 156.7, 156.5, 138.6, 135.6, 134.2, 132.8, 128.9, 125.6, 122.8, 117.7, 87.2, 79.8, 73.5, 55.0, 43.2,

40.8, 37.3, 31.0, 30.7, 30.4, 26.2, 19.2, 18.0, 12.3. MS (ESI): calculated for $[M + 2Na]^{++}$ *m/z* = 1365.7, found *m/z* = 1366.7.

25,26,27,28-Tetrakis{3-[(Nα-Cbz-L-Arg)amino]propoxy}calix[4]arene, tetrahydrochloride (67a).

The reaction was stopped by evaporation of methanol under reduced pressure. The crude material was further purified by a trituration in diethyl ether (5 mL), dissolved in MeOH (5 ml) and applied onto ammonium ion exchange cartridges.

^{1}H NMR (300 MHz, CD_3OD) δ 7.96 (s, 4H, CH_2NHCO), 7.42-7.20 (m, 15H, Ar*H*Cbz), 6.70-6.42 (m, 12H, Ar*H*), 5.15-4.93 (m, 8H, CH_2Cbz), 4.37 (d, *J* = 13.1 Hz, 4H, $ArCH_2Ar$), 4.26-4.09 (m, 4H, COC*H*NH), 4.00-3.76 (m, 8H, OCH_2), 3.50-3.31 (m, 8H, $OCH_2CH_2CH_2$), 3.25-3.03 (m, 12H, $ArCH_2Ar$ and CH_2NHCNH), 2.28-2.00 (m, 8H, OCH_2CH_2), 2.00-1.49 (m, 16H, $COCHCH_2CH_2CH_2NH$). MS (ESI): calculated for $[M + 2Na]^{++}$ *m/z* = 1835.9, found *m/z* = 1836.7.

25,26,27,28-Tetrakis{3-[(Nα-Cbz-Nω-N'ω-$(Cbz)_2$-L-Arg)amino]propoxy}calix[4]arene (67b).

The crude material was purified by preparative TLC (eluent: dichloromethane/ethyl acetate= 6:1) to obtain the pure product as a white solid in 20% yield.

^{1}H NMR (300 MHz, CD_3Cl_3/CD_3OD= 19:1) δ 7.27-6.95 (m, 60H, Ar*H* Cbz), 6.59-6.21 (m, 12H, Ar*H*), 5.13-4.68 (m, 24H, CH_2Cbz), 4.20-3.48 (m, 24H, $ArCH_2Ar$, COC*H*NH, OCH_2 and $OCH_2CH_2CH_2$), 3.35-2.88 (m, 12H, CH_2NHCNH and $ArCH_2Ar$), 1.77 (bs, 8H, OCH_2CH_2), 1.49 (bs, 16H, $COCHCH_2CH_2CH_2NH$). ^{13}C NMR (75 MHz, CD_3Cl_3/CD_3OD= 19:1) δ 172.3, 163.3, 160.2, 156.4, 155.4, 136.1, 134.4, 128.5, 128.2, 127.7, 123.0, 122.1, 72.3, 68.7, 66.9, 66.6, 54.3, 48.8, 48.5, 44.2, 36.7, 30.6, 29.7, 29.5, 28.7, 24.7. MS (ESI): calculated for $[M + 2Na]^{++}$ *m/z* = 1465.6, found *m/z* = 1465.4.

Bis{2-[3-(Nα-Boc-Nω-Pbf-L-Arg)-amino]propoxy-3-methylphenyl}methane (68).

The crude material was purified by preparative TLC (eluent: ethyl acetate/hexane= 9:1) to obtain the pure product as a colourless oil in 21% yield.

^{1}H NMR (300 MHz, CD_3CN): δ 7.13 (bt, 2H, N*H*COCH), 7.02 (dd, 2H, *J* = 7.4, 1.3 Hz, Ar*H*), 6.89 (t, 2H, *J* = 7.4 Hz, Ar*H*), 6.82 (dd, 2H, *J* = 7.4, 1.3 Hz, Ar*H*), 6.10 (bs, N*H*CN*H*N*H*), 5.70 (bs, 2H, *H*NCOO), 3.97 (bs, 4H, $ArCH_2Ar$, NHCOC*H*), 3.73 (t, *J* = 6.3

Hz, 4H, OCH_2), 3.45-3.20 (m, 4H, $OCH_2CH_2CH_2$), 3.20-2.95 (m, 4H, N=CNHCH_2), 2.96 (s, 4H, CH_2Pbf), 2.52 (s, 6H, CH_3Pbf), 2.45 (s, 6H, CH_3Pbf), 2.22 (s, 6H, CH_3Pbf), 2.03 (s, 6H, ArCH_3), 1.98-1.82 (m, 4H, OCH_2CH_2), 1.75-1.30 (m, 8H, $N=CNHCH_2CH_2CH_2$), 1.41 (s, 18H, *t*Bu), 1.34 (s, 12H, $C(CH_3)_2$Pbf). ^{13}C NMR (75 MHz, CD_3CN): δ 173.1, 158.9, 157.1, 156.3, 156.2, 138.6, 134.7, 134.3, 132.8, 131.7, 129.9, 128.9, 125.6, 124.4, 87.1, 79.6, 71.0, 54.8, 43.2, 40.7, 37.1, 30.6, 30.2, 29.9, 28.3, 28.2, 26.1, 19.2, 17.9, 16.3, 12.3. MS (ESI): calculated for $[M + Na]^+$ *m/z* = 1381.7, found *m/z* 1382.3.

General procedure for Fmoc deprotection: a solution of Fmoc protected upper or lower rim calix[4]arene (10 μmol) in piperidine/dry DCM (20% v/v, 1.5 mL) was stirred at rt, and checked by mass spectroscopy. After completion (24 h), the reaction was quenched with water (2 mL) and the organic phase dried over anhydrous Na_2SO_4 and concentrated under reduced pressure. The crude material was precipitated with hexane, washed and centrifuged several times to remove dibenzofulvene and dibenzofulvene-piperidine adduct thus obtaining a white solid used without further purification.

5,11,17,23-Tetrakis[Nω-Mtr-L-Arg-amino]-25,26,27,28-tetrakis(*n*-hexyloxy)calix[4]arene (58).

MS (ESI): calculated for $[M + 3H]^{+++}$ *m/z* = 765.4, found *m/z* 765.9.

25,26,27,28-Tetrakis{3-[Nω-Mtr-L-Arg]aminopropoxy}calix[4]arene (65).

MS (ESI): calculated for $[M + 2Na]^{++}$ *m/z* = 1085.5, found *m/z* 1086.0.

General procedure for Pbf and Mtr deprotection: a solution of upper or lower rim calix[4]arene or linear compound (15 μmol) in TFA/TIS/H_2O (95/5/5, 5 mL) was stirred at room temperature. The progression of the reaction was followed using mass spectroscopy. After completion (2-24 h), the volatiles were removed under reduced pressure and the residue washed with ethyl acetate (3×5 mL) to remove the exceeding TFA. The crude material was precipitated, washed and centrifuged with anhydrous diethyl ether (3×7 mL). The trifluoroacetate anion of the resulting TFA salts was exchanged by adding 10 mM HCl solution (3×5 mL) followed by evaporation under reduced pressure.

5,11,17,23-Tetra(L-Arg-amino)-25,26,27,28-tetrakis(*n*-hexyloxy)calix[4]arene, octa-hydrochloride (59).

Crude compound **57b** (8 mg, 4.6 μmol) was dissolved in 10 mM HCl (5 mL) and washed with CH_2Cl_2 (5 mL). The exceeding HCl was removed under reduced pressure. The crude compound was dissolved in water (2 mL) and TFA (4 μL) and purified by semi-preparative RP-HPLC using a C_{12} column (separation conditions were studied on an analytical phenyl and an analytical C_{12} columns).

- **Column:** semi-preparative "Jupiter 4u Proteo 90A" C_{12}
- **Particles diameter:** 4 μm
- **Porosity:** 90Å
- **Dimensions:** 250×10 mm
- **Detector:** UV-visible at λ= 254 nm
- **Eluents mixture:** A: 100% H_2O + 0.05% TFA
  B: 100% CH_3CN + 0.05% TFA
- **Injection volume:** 300 μL
- **Gradient:**

Time (min)	Flow	%A	%B
-	4.00 mL/min	70%	30%
20	4.00 mL/min	40%	60%
25	4.00 mL/min	40%	60%

- **Retention time:** 13.646 min

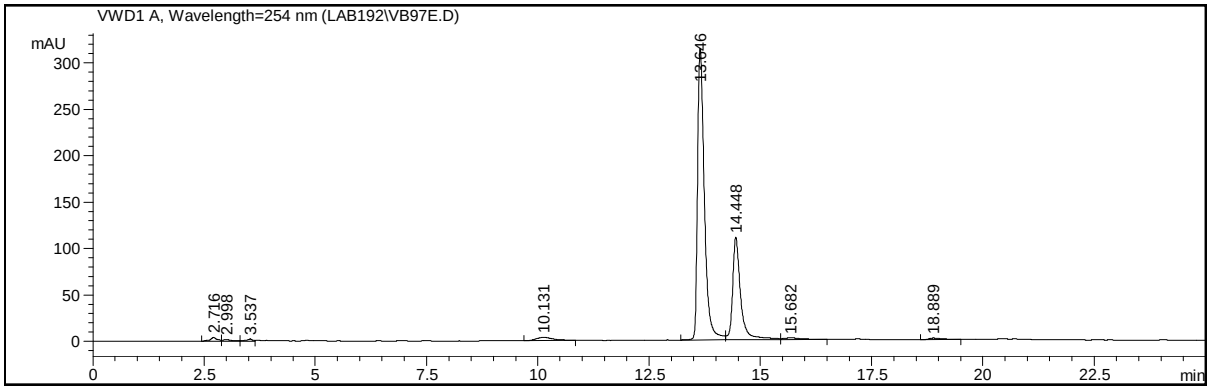

Tests with analytical C_{12} and phenyl columns.

- **Column:** analytical phenyl "Synergi 4u POLAR-RP 80A"
- **Particles diameter:** 4 μm
- **Porosity:** 80A
- **Dimensions:** 150×4.6 mm
- **Detector:** UV-visible at λ= 254 nm
- **Eluents mixture:** A: 100% H_2O + 0.05% TFA
  B: 100% CH_3CN + 0.05% TFA
- **Injection Volume:** 5 μL
- **Gradient:**

Time (min)	Flow	%A	%B
-	4.00 mL/min	70%	30%
20	4.00 mL/min	40%	60%
25	4.00 mL/min	40%	60%

- **Retention time:** 9.266 min

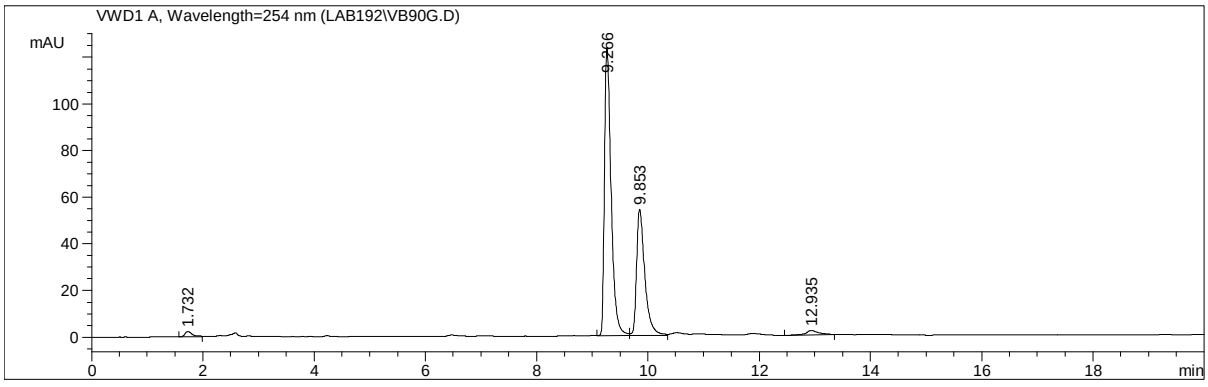

- **Column:** analytical C_{12} "Jupiter 4u Proteo 90A"
- **Particles diameter:** 4 μm
- **Porosity:** 90 A
- **Dimensions:** 250×4.6 mm
- **Detector:** UV-visible at λ= 254 nm
- **Eluents mixture:** A: 100% H_2O + 0.05% TFA

B: 100% CH_3CN + 0.05% TFA

- **Injection Volume:** 5 μL
- **Gradient:**

Time(min)	Flow	%A	%B
-	4.00 mL/min	70%	30%
20	4.00 mL/min	40%	60%
25	4.00 mL/min	40%	60%

- **Retention time:** 16.176

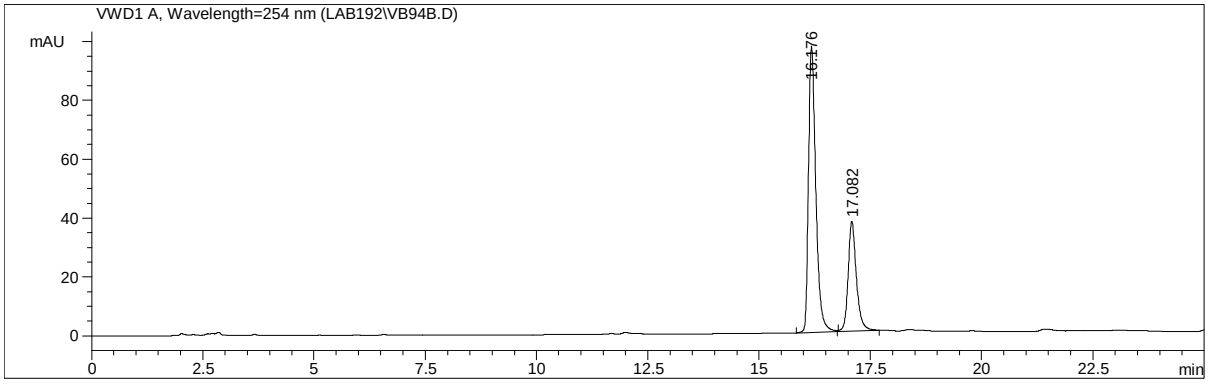

The fractions corresponding to the major component were collected and the solvent removed under reduced pressure. The residue was treated with a 10 mM HCl solution (3×5 mL) and each time the volatiles were removed under reduced pressure in order to get rid of the TFA. ^{1}H NMR (300 MHz, CD_3OD) δ 7.18 (s, 4H, Ar*H*), 6.87 (s, 4H, Ar*H*), 4.47 (d, *J* = 12.9 Hz, 4H, ArC*H*$_2$Ar), 4.06 (bs, 4H, COC*H*NH_3^+), 3.90 (t, *J* = 7.3 Hz, 8H, OC*H*$_2$), 3.40-3.20 (m, 8H, C*H*$_2$NH), 3.16 (d, *J* = 12.9 Hz, 4H, ArC*H*$_2$Ar), 1.98 (bs, 16H, OCH_2CH_2 and $COCHCH_2$), 1.72 (bs, 8H, $COCHCH_2CH_2$), 1.50-1.20 (m, 24H, $OCH_2CH_2CH_2CH_2CH_2$), 0.94 (t, *J* = 6.3 Hz, 12H, C*H*$_3$). ^{1}H NMR (300 MHz, D_2O) δ 7.28 (bs, 4H, Ar*H*), 6.88 (bs, 4H, Ar*H*), 4.30 (bs, 4H, ArC*H*$_2$Ar), 4.11 (bs, 4H, COC*H*NH_3^+), 3.76 (bs, 8H, OC*H*$_2$), 3.40-2.89 (bs, 12 H, C*H*$_2$NH and ArC*H*$_2$Ar), 1.92 (bs, 16H, OCH_2CH_2 and $COCHCH_2$), 1.65 (bs, 8H, $COCHCH_2CH_2$), 1.34 (m, 24H, $OCH_2CH_2CH_2CH_2CH_2$), 0.90 (t, 12H, C*H*$_3$). ^{13}C NMR (75 MHz, CD_3OD) δ 167.9, 158.9, 155.1, 136.6, 136.5, 133.2, 122.6, 122.1, 77.0, 54.8, 42.2, 33.7, 32.4, 31.8, 30.2, 27.6, 25.9, 24.3, 14.8. MS (ESI): calculated for $[M + 2H - 8HCl]^{++}$ *m/z* = 723.5, found *m/z* 723.7.

5,11,17,23-Tetrakis(L-Arg-amino)-25,26,27,28-tetrakis(*n*-ethoxyethoxy)calix[4]arene octa-hydrochloride (63).

The pure product was obtained as a white solid in 80% yield.

^{1}H NMR (300 MHz, CD_3OD) δ 7.15 (bs, 4H, Ar*H*), 6.98 (bs, 4H, Ar*H*), 4.57 (d, *J* = 12.5 Hz, 4H, ArC*H*$_2$Ar), 4.13 (bs, 8H, ArOC*H*$_2$), 4.10 (bs, 4H, C*H*CONH), 3.94-3.85 (m, 8H, $ArOCH_2CH_2$), 3.56 (q, *J* = 6.9 Hz, 8H, $ArOCH_2CH_2OCH_2$), C*H*$_2$NH under the CD_3OD signal, 3.14 (d, *J* = 12.5 Hz, 4H, ArC*H*$_2$Ar), 2.15-1.62 (m, 16H, $COCHCH_2CH_2$), 1.20 (t, *J* = 6.9 Hz, 12H, CH_2CH_3). ^{1}H NMR (300 MHz, D_2O) δ 7.18 (d, *J* = 1.6 Hz, 4H, Ar*H*), 7.04 (d, *J* = 1.6 Hz, 4H, Ar*H*), 4.55 (d, *J* = 12.9 Hz, 4H, ArC*H*$_2$Ar), 4.26 (t, *J* = 4.8 Hz, 8H, ArOC*H*$_2$), 4.14 (t, *J* = 6.0 Hz, 4H, C*H*CONH), 3.99 (t, *J* = 4.8 Hz, 8H, $ArOCH_2CH_2$), 3.64 (q, *J* = 6.9 Hz, 8H, $ArOCH_2CH_2OCH_2$), 3.64 (d, *J* = 12.9 Hz, 4H, ArC*H*$_2$Ar), 3.34-3.14 (m, 8H, C*H*$_2$NH), 2.14-1.86 (m, 16H, $COCHCH_2CH_2$), 1.19 (t, *J* = 6.9 Hz, 12H, CH_2CH_3).

^{13}C NMR (75 MHz, CD_3OD) δ 167.7, 156.6, 153.4, 135.3, 131.3, 122.2, 121.9, 73.0, 69.8, 66.5, 53.2, 40.1, 30.5, 27.7, 23.1, 14.2. MS (ESI): calculated for $[M + 4H - 8HCl]^{4+}$ *m/z* = 350.2, found *m/z* = 350.5.

25,26,27,28-Tetrakis[3-(L-Arg-amino)propoxy]calix[4]arene, octa-hydrochloride (66).

The calix[4]arene **67a** (80 mg, 27.7 μmol) was dissolved in MeOH (10 mL). A catalytic amount of Pd/C was added and hydrogenation was carried out at 2 atm in a Parr reactor for 24 h. Progression of the reaction was followed by ^{1}H NMR and ESI-MS. The catalyst was filtered off and the solvent removed under reduced pressure. The residue was treated with HCl 0.5 M in MeOH until pH 3 (xx mL) which then was removed at the rotavapor. The final product was obtained with some impurities originating from the previous reaction and it needed to be further purify by reverse-phase chromatography or by HPLC.

^{1}H NMR (300 MHz, CD_3OD) δ 6.70-6.43 (m, 12H, Ar*H*), 4.32 (d, *J* = 12.9 Hz, 4H, ArC*H*$_2$Ar), 4.20-3.86 (m, 12H, COC*H*NH and OC*H*$_2$), 3.65-3.40 (bt, 8H, $OCH_2CH_2CH_2$), 3.40-3.27 (m, 8H, C*H*$_2$NHCNH), 3.18 (d, *J* = 12.9 Hz, 4H, ArC*H*$_2$Ar), 2.35-2.10 (m, 8H, OCH_2CH_2), 2.10-1.60 (m, 16H, $COCHCH_2CH_2CH_2NH$). ^{1}H NMR (300 MHz, D_2O) δ 6.84 (d, *J* = 7.4 Hz, 8H, Ar*H*), 6.70 (t, *J* = 7.4 Hz, 4H, Ar*H*), 4.40 (d, *J* = 13.0 Hz, 4H, ArC*H*$_2$Ar), 4.16-3.90 (m, 12H, COC*H*NH and OC*H*$_2$), 3.72-3.55 (m, 4H, OCH_2CH_2CH*H*), 3.48-3.15 (m, 16H, OCH_2CH_2CH*H*, ArC*H*$_2$Ar and C*H*$_2$NHCNH), 2.40-2.15 (m, 8H, OCH_2CH_2), 2.10-1.85

(m, 8H, COCHCH_2), 1.77-1.56 (m, 8H, COCHCH$_2$CH_2). MS (ESI): calculated for [M + 2H - 8HCl]$^{++}$ *m/z* = 639.4, found *m/z* = 640.0.

Bis-{2-[3-(L-Arg-amino)propoxy]-3-methylphenyl}methane, tetra-hydrochloride (69). The pure product was obtained as a light yellow oil in 85% yield.

^{1}H NMR (300 MHz, CD_3OD): δ 7.03 (d, *J* = 6.9 Hz, 2H, Ar*H*), 6.90 (t, *J* = 6.9 Hz, 2H, Ar*H*), 6.82 (d, *J* = 6.9 Hz, 2H, Ar*H*), 4.02 (s, 2H, ArCH_2Ar), 3.95 (bs, 2H, COC*H*), 3.78 (bt, 4H, OCH_2), 3.46 (bs, 4H, OCH$_2$CH$_2$CH_2), 3.22 (bs, 4H, N=CNHCH_2), 2.28 (s, 6H, ArCH_3), 2.03-1.58 (bm, 12H, OCH$_2$CH_2 and COCHCH_2CH_2). ^{1}H NMR (300 MHz, D_2O): δ 7.18 (d, *J* = 7.5 Hz, 2H, Ar*H*), 7.05 (t, *J* = 7.5 Hz, 2H, Ar*H*), 6.95 (d, *J* = 7.5 Hz, 2H, Ar*H*), 4.02 (s, 2H, ArCH_2Ar), 3.95 (t, 2H, *J* = 6.6 Hz, COC*H*), 3.83 (t, 4H, *J* = 6.3 Hz, OCH_2), 3.56-3.45 (m, 2H, OCH$_2$CH$_2$CH*H*), 3.38-3.26 (m, 2H, OCH$_2$CH$_2$C*H*H), 3.12 (t, 4H, *J* = 6.9 Hz, N=CNHCH_2), 2.27 (s, 6H, ArCH_3), 2.08-1.93 (m, 4H, OCH$_2$CH_2), 1.93-1.83 (m, 4H, CHCH_2), 1.66-1.54 (m, 4H, COCHCH$_2$CH_2). ^{13}C NMR (75 MHz, CD_3OD) δ 170.3, 158.9, 157.1, 135.4, 132.4, 130.7, 129.9, 125.4, 71.6, 54.4, 42.0, 38.6, 31.4, 30.9, 30.1, 25.7, 17.0. MS (ESI): calculated for [M + H - 4HCl]$^+$ *m/z* = 655.4, found *m/z* 655.6.

DNA preparation and storage. Plasmid DNA was purified through cesium chloride gradient centrifugation.[54] A stock solution of the plasmid 0.35 μM in milliQ water (Millipore Corp., Burlington, MA) was stored at -20 °C.

Electrophoresis mobility shift assay (EMSA)

Binding reactions were performed in a final volume of 14 μL with 10 μL of 20 mM Tris/HCl pH 8, 1 μL of plasmid (1 μg of pEGFP-C1) and 3 μL of compound at different final concentrations, ranging from 25 to 200 μM. Binding reaction was left to take place at room temperature for 1 h; 5 μL of 1 g/mL in H_2O of glycerol was added to each reaction mixture and loaded on a TA (40 mM Tris-Acetate) 1% agarose gel. At the end of the binding reaction 1 μL (0.01 mg) of ethidium bromide solution is added. The gel was run for 2.5 h in TA buffer at 10 V/cm. EDTA was omitted from the buffers because it competes with DNA in the reaction.

Sample preparation and AFM imaging. DNA samples were prepared by diluting the plasmid DNA to a final concentration of 0.5 nM in deposition buffer (4 mM Hepes, 10 mM NaCl, 2 mM $MgCl_2$, pH = 7.4) either in the presence or absence of ligands. When needed, ethanol at a defined concentration was added to the deposition buffer prior to addition of

DNA and calixarenes. The mixture was incubated for 5 min at room temperature, then a 20 μL droplet was deposited onto freshly-cleaved ruby mica (Ted Pella, Redding, CA) for 1.5 min. The mica disk was rinsed with milliQ water and dried with a weak nitrogen stream. AFM imaging was performed on the dried sample with a Nanoscope IIIA Microscope (Digital Instruments Inc. Santa Barbara, CA) operating in tapping mode. Commercial diving board silicon cantilevers (NSC-15 Micromash Corp., Estonia) were used. Images of 512×512 pixels were collected with a scan size of 2 μm at a scan rate of 3-4 lines per second and were flattened after recording using Nanoscope software.

Cell culture and transient transfection assay. The human rhabdomyosarcoma cell line RD-4, obtained from David Derse, National Cancer Institute, Frederick, Maryland, was maintained as a monolayer using growth medium containing 90% DMEM, 10% FBS, 2 mM l-glutamine, and 100 IU/mL penicillin, 10 μg/mL streptomycin. Cells were subcultured to a fresh culture vessel when growth reached 70-90% confluence (i.e. every 3-5 days) and incubated at 37 °C in a humidified atmosphere of 95% air-5% CO_2. Transfections were performed in 6 well plates, when cells were 80% confluent (approximately 3×105 cells) on the day of transfection. 3 μg of plasmid, and different concentration of ligands were added to 1 mL of serum-free medium, mixed rapidly and incubated at room temperature for 20 min. Each mixture was carefully added to the cells following the removal of the culture medium from the cells. Lipoplex formulations were performed adding DOPE to plasmid-ligand mixture at 1: 2 ligand: DOPE molar ratio, where ligand concentration was kept to 10 μM. LTX™ transfection reagent was used according to manufacturer's protocol as positive transfection control. The mixture and cells were incubated at 37 °C in a humidified atmosphere of 95% air-5% CO_2 for 5 h. Finally, transfection mixture was removed and 3 mL of growth medium added to each transfected well and left to incubate for 72 h. Five fields were randomly selected from each well without viewing the cells (one in the centre and one for each quadrant of the well) and examined. The transfected cells were observed under fluorescence microscope for EGFP expression. Each experiment was done three times. Statistical differences between treatments were calculated with Student's test and multifactorial ANOVA.

Vero (African green monkey, ATCC CRL-1586), BoMac (bovine macrophage, obtained from J. Stabel, National Animal Disease Center, Ames, IA, USA), N2a (Mouse neuroblastoma, ATCC CCL-131), AUBEK (bovine foetal kidney cell line, ATCC CCL 163) and hMSC (human mesenchymal stem cells, obtained from R. Sala, University of Parma, Italy) were

grown in EMEM medium containing NEAA, 10% FBS, 2 mM l-glutamine, 100 IU/mL penicillin and 100 μg/mL streptomycin. All cultures were incubated at 37 °C in a humidified atmosphere containing 5% CO_2. Transfection were performed as described for RD-4 cells.

MTT survival assay for cell viability determination. Following transfection, complete medium (90% DMEM, 10% FBS, 2 mM l-glutamine, and 100 IU/mL penicillin, 10 μg/mL streptomycin) containing MTT (5 mg/mL) was added to the culture for 4 h. Then, after the addition of an equal volume of solubilisation solution (10% SDS in HCl 0.01 M) cells were incubated at 37 °C overnight. Specific optical density was measured at 540 nm, using 690 nm as reference wavelength in an SLT-Lab microreader (Salzburg, Austria). Each experiment was done three times and each treatment was performed with eight replicates. Statistical differences among treatments were calculated with Student's test and multifactorial ANOVA.

4.5 References

1. Schug, K. A.; Lindner, W. *Chem. Rev.* **2005**, *105*, 67-113.

2. Mehrotra, M. M.; Sternbach, D. D.; Rodriguez, M.; Charifson, P.; Berman, J. *Bioorg. Med. Chem. Lett.* **1996**, *6*, 1941-1946.

3. a) Ma, J. C.; Dougherty, D. A. *Chem. Rev.* **1997**, *97*, 1303-1324; b) Zacharias, N.; Dougherty, D. A. *Trends Pharmacol. Sci.* **2002**, *23*, 281-287.

4. Blondeau, P.; Segura, M.; Perez-Fernandez R.; de Mendoza, J. *Chem. Soc. Rev.* **2007**, *36*, 198-210.

5. Bogan, A. S.; Thorn, K. S. *J. Mol. Biol*. **1998**, *280*, 1-9.

6. Woods, A. S.; Ferre, S. J. *Proteome Res.* **2005**, *4*, 1397-1402.

7. Ruoslahti, E. *Annu. Rev. Cell Dev. Biol.* **1996**, *12*, 697-715.

8. Humphries, M. J. *Biochem. Soc. Trans.* **2000**, *4*, 311-339.

9. Hah, J.-M.; Roman, L. J.; Martasek, P.; Silverman, R. B. *Journal of medicinal chemistry*, **2001**, *44*, 2667-2670.

10. García-Pérez, M.; Pinto, M.; Subirana, J. A. *Biopolymers* **2003**, *69*, 432-439.

11. Zhang, Y.; Reinberg, D. *Genes Dev.* **2001**, *15*, 2343-2360.

12. a) Frankel, A. D.; Pabo, C. O. *Cell* **1988**, *55*, 1189-1193; b) Green, M.; Loewenstein, P. M. *Cell* **1988**, *55*, 1179-1188.

13. Frankel, A. D.; Young, J. A. *Annu. Rev. Biochem.* **1998**, *67*, 1-25.

14. Fawell, S.; Seery, J.; Daikh, Y.; Moore, C.; Chen, L. L.; Pepinsky, B.; Barsoum, J. *PNAS* **1994**, *91*, 664-668.

15. Vivès, E.; Brodin, P.; Lebleu, B. *J. Biol. Chem.* **1997**, *272*, 16010-16017.

16. a) Nagahara, H.; Vocero-Akbani, A. M.; Snyder, E. L.; Ho, A.; Latham, D. G.; Lissy, N. A.; Becker-Hapak, M; Ezhevsky, S. A.; Dowdy, S. F. *Nat. Med.* **1998**, *4*, 1449-1452; b) Vocero-Akbani, A. M.; Heyden, N. V.; Lissy, N. A.; Ratner, L.; Dowdy, S. F. *Nat. Med.* **1999**, *5*, 29-33.

17. Nakase, I.; Takeuchi, T.; Tanaka, G.; Futaki, S. *Adv. Drug. Deliv. Rev.* **2008**, *60*, 598-607.

18. a) Langel, Ü. (Ed.), Handbook of Cell-Penetrating Peptides, Second Edition, CRC Press, Boca Raton, **2006**; b) Rothbard, J. B.; Garlington, S.; Lin, Q.; Kirschberg, T.; Kreider, E.; McGrane, P. L.; Wender, P. A.; Khavari, P. A. *Nat. Med.* **2000**, *6*, 1253-1257; c) Rothbard, J. B.; Jessop, T. C.; Lewis, R. S.; Murray, B. A.; Wender, P. A. *J. Am. Chem. Soc.* **2004**, *126*, 9506-9507; d) Rothbard, J. B.; Kreider, E.; VanDeusen, C. L.; Wright, L.; Wylie, B. L.; Wender, P. A. *J. Med. Chem.* **2002**, *45*, 3612-3618.

19. a) Mitchell, D. J.; Kim, D. T.; Steinman, L.; Fathman, C. G.; Rothbard, J. B. *J. Pept. Res.* **2000**, *56*, 318-325; b) Wender, P. A.; Mitchell, D. J.; Pattabiraman, K.; Pelkey, E. T.; Steinman, L.; Rothbard, J. S. *PNAS* **2000**, *97*, 13003-13008.

20. Futaki, S.; Suzuki, T.; Ohashi, W.; Yagami, T.; Tanaka, S.; Ueda, K.; Sugiura, Y. *J. Biol. Chem.* **2001**, *276*, 5836-5840.

21. Umezawa, N.; Gelman, M. A.; Haigis, M. C.; Raines, R. T.; Gellman, S. H. *J. Am. Chem. Soc.* **2002**, *124*, 368-369.

22. Sakai, N.; Matile, S. *J. Am. Chem. Soc.* **2003**, *125*, 14348-14356.

23. Torchilin, V. P.; Rammohan, R.; Weissig, V.; Levchenko, T. S. *PNAS* **2001**, *98*, 8786-8791.

24. Bullok, K. E.; Dyszlewski, M.; Prior, J. L.; Pica, C. M.; Sharma, V.; Piwnica-Worms, D. *Bionconjugate Chem.* **2002**, *13*, 1226-1237.

25. Aime, S.; Botta, M.; Garino, E.; Geninatti Crich, S.; Giovenzana, G.; Pagliarin, R.; Palmisano, G.; Sisti, M. *Chem. Eur. J.* **2000**, *6*, 2609-2617.

26. Wright, L. R.; Rothbard, J. B.; Wender, P. A. *Curr. Protein Pept. Sci.* **2003**, *4*, 105-124.

27. a) Silphaduang, U.; Noga, E. J. *Nature* **2001**, *414*, 268-269; b) Zasloff, M. *Nature* **2002**, *415*, 389-395; c) Strom, M. B.; Rekdal, O.; Svendsen, J. S. *J. Pept. Sci.* **2002**, *8*, 431-437.

28. Doyle, S. R.; Chan, C. K. *Genetics Vaccines and Therapy*, **2007**, *5*.

29. Dufes, C.; Uchegbu, I. F.; Schaetzlein, A. G. *Advanced Drug Delivery Reviews*, **2005**, *57*, 2177-2202.

30. Takeuchi, T.; Kosuge, M.; Tadokoro, A.; Sugiura, Y.; Nishi, M.; Kawata, M.; Sakai, N.; Matile, S.; Futaki, S. *ACS Chemical Biology* **2006**, *1*, 299-303.

31. Lundin, K. E.; Hasan, M.; Moreno, P. M.; Toernquist, E.; Oprea, I.; Svahn, M. G.; Simonson, E. O.; Smith, C. I. E. *Biomolecular Engineering* **2005**, *22*, 185-192.

32. Wettig, D.; Badea, I.; Donkuru, M.; Verrall, R. E.; Foldvari, M. *J. Gene Med.* **2007**, *9*, 649-658.

33. Akine, A.; Thomas, M.; Klibanov, A. M.; Langer, R. *Journal of Gene Medicine* **2005**, *7*, 657-663.

34. Behr, J. P. *CHIMIA International Journal for Chemistry* **1997**, *51*, 1-2, 34-36.

35. Gutsche, C. D. Calixarenes, The Royal Society of Chemistry (Ed.: Stoddart, J. F.), Cambridge, **1989**.

36. a) Sansone, F.; Barboso, S.; Casnati, A.; Fabbi, M.; Pochini, A.; Ugozzoli, F.; Ungaro, R. *Eur. J. Org. Chem.* **1998**, 897-905; b) Casnati, A.; Fabbi, M.; Pelizzi, N.; Pochini, A.; Sansone, F.; Ungaro, R.; Di Modugno, E.; Tarzia, G. *Bioorg. Med. Chem. Lett.* **1996**, *6*, 2699-2704.

37. Lazzarotto, M.; Sansone, F.; Baldini, L.; Casnati, A.; Cozzini, P.; Ungaro, R. *Eur. J. Org. Chem.* **2001**, *3*, 595-602.

38. Baldini, L.; Casnati, A.; Sansone, F.; Ungaro, R. *Calixarenes in the Nanoworld*, Editors Jacques Vicens, Jack Harrowfield, **2007**, *12*, 231-257.

39. Mammen, M.; Choi, S.-K.; Whitesides, G. M. *Angew. Chem. Int. Engl. Ed.* **1998**, *37*, 2755-2794.

40. Baldini, L.; Sansone, F.; Scaravelli, F.; Massera, C.; Casnati, A.; Ungaro, R. *Tetrahedron letters* **2009**, *50*, 3450-3453.

41. Smukste, I.; House, B. E.; Smithrud, D. B. *J. Org. Chem.* **2003**, *68*, 2559-2571.

42. Martos, V.; Bell, S. C.; Santos, E.; Isacoff, E. Y.; Trauner, D.; de Mendoza, J. *PNAS* **2009**, *106*, 10482-10486.

43. Hille, B. *Ion Channels of Excitable Membranes*, **2001** (Sinauer, Sunderland, MA).

44. Ashcroft, F. M. *Ion Channels and Disease: Channelopathies* **2000** (Academic, San Diego).

45. Radau, G. *Monatshefte fur Chemie* **2003**, *134*, 1033-1036.

46. Zhou, P.; Dragulescu-Andrasi, A.; Birendra Bhattacharya, B.; O'Keefe, H.; Vatta, P.; Hyldig-Nielsen, J.; Ly, D. H. *Bioorganic & Medicinal Chemistry Letters* **2006**, *16*, 4931-4935.

47. Schazmann, B.; Mcmahon, G.; Nolan, K.; Diamond, D. *Supramolecular Chemistry* **2005**, *17*, 393-399; b) Schazmann, B.; Alhashimy, N.; Diamond, D. *J. Am. Chem. Soc.* **2006**, *128*, 8607-8614.

48. Budka, J.; Curinova, P.; Gu, R.; Lhotak, P.; Stibor, I.; Schraml, J.; Dehaen, W. *Naturforsch.* **2007**, *62b*, 439-446.

49. a) Casado, F.; Pisano, L.; Farriol, M.; Gallardo, I.; Marquet, J.; Melloni, G. *J. Org. Chem.* **2000**, *65*, 322-331; b) Bachelet, J. P.; Demerseman, P.; Royer, R. *Bulletin de la Societe Chimique de France* **1974**, *11*, 2631-2634.

50. Sansone, F.; Dudic, M.; Donofrio, G.; Rivetti, C.; Baldini, L.; Casnati, A.; Cellai, S.; Ungaro, R. *J. Am. Chem. Soc.* **2006**, *128*, 14528-14536.

51. Mislin, G.; Graf, E.; Hosseini, M. W. *Tetrahedron Lett.*, **1996**, *37*, 4503-4506.

52. Della Ca', N.; Fontanella, M.; Sansone, F.; Ugozzoli, F.; Ungaro, R.; Liger, K; Dozol, J.-F. *Eur. J Org. Chem.* **2005**, *11*, 2338-2348.

53. Consoli, G. M. L.; Cunsolo, F.; Geraci, C.; Sgarlata, V. *Org. Lett.*, **2004**, *6*, 4163-4166.

54. Maniatis, T.; Fritsch, E. F.; Sambrook, J. in *Molecular Cloning: A Laboratory Manual*, 2nd edition, **1989**, Cold Spring Harbor Laboratory: New York.